Nat. Hazards Earth Syst. Sci., 20, 3057–3082, 2020
https://doi.org/10.5194/nhess-20-3057-2020

Natural Hazards and Earth System Sciences
Open Access
EGU

Evaluation of EURO-CORDEX (Coordinated Regional Climate Downscaling Experiment for the Euro-Mediterranean area) historical simulations by high-quality observational datasets in southern Italy: insights on drought assessment

David J. Peres[1], Alfonso Senatore[2], Paola Nanni[1], Antonino Cancelliere[1], Giuseppe Mendicino[2], and Brunella Bonaccorso[3]

[1]Department of Civil Engineering and Architecture, University of Catania, Catania, 95123, Italy
[2]Department of Environmental Engineering, University of Calabria, Arcavacata di Rende (CS), 87036, Italy
[3]Department of Engineering, University of Messina, St Agata, Messina, 98166, Italy

Correspondence: Alfonso Senatore (alfonso.senatore@unical.it)

Received: 12 March 2020 – Discussion started: 25 March 2020
Revised: 21 September 2020 – Accepted: 2 October 2020 – Published: 14 November 2020

Abstract. Many recent studies indicate climate change as a phenomenon that significantly alters the water cycle in different regions worldwide, also implying new challenges in water resource management and drought risk assessment. To this end, it is of key importance to ascertain the quality of regional climate models (RCMs), which are commonly used for assessing at proper spatial resolutions future impacts of climate change on hydrological events. In this study, we propose a statistical methodological framework to assess the quality of the EURO-CORDEX RCMs concerning their ability to simulate historic climate (temperature and precipitation, the basic variables that determine meteorological drought). We then specifically focus on drought characteristics (duration, accumulated deficit, intensity, and return period) determined by the theory of runs at seasonal and annual timescales by comparison with high-density and high-quality ground-based observational datasets. In particular, the proposed methodology is applied to the Sicily and Calabria regions (southern Italy), where long historical precipitation and temperature series were recorded by the ground-based monitoring networks operated by the former Regional Hydrographic Offices, whose density is considerably greater than observational gridded datasets available at the European level, such as E-OBS or CRU-TS. Results show that among the more skilful models able to reproduce, overall, precipitation and temperature variability as well as drought characteristics, many are based on the CLM-Community RCM, particularly in combination with the HadGEM2 global circulation model (GCM). Nevertheless, the ranking of the models may slightly change depending on the specific variable analysed as well as the temporal and spatial scale of interest. From this point of view, the proposed methodology highlights the skills and weaknesses of the different configurations and can serve as an aid for selecting the most suitable climate model for assessing climate change impacts on drought processes and the underlying variables.

1 Introduction

A growing number of scientific studies claim that climate change due to global warming will significantly alter the water cycle, with an increase in the intensity and frequency of extreme hydro-climatic events in several areas around the globe (Arnell et al., 2001; Huntington, 2006; IPCC, 2014, 2018). These include the Mediterranean region, which is recognized as one of the major hot spots of climate change due to future projections of temperature increase and annual precipitation decrease (Giorgi, 2006; Kjellström et al., 2013), which determines a potential increase in drought frequency and severity.

Global circulation and regional climate models (GCMs and RCMs) can play a crucial role in understanding the

potential spatio-temporal evolution of climate change in the future, thus improving current monitoring and planning tools (e.g. Mendicino and Versace, 2007; Hart and Halden, 2019) and supporting decision-makers in choosing and implementing the best solutions to minimize the impact of climate change on human systems and the environment at the regional scale. While GCM simulations describe climate evolution at a large scale by using coarse-resolution information, RCM simulations, derived through climate-downscaling techniques, aim to represent regional- and local-scale weather conditions with grid resolutions lower than 50 km, down to about 10 km (Kotlarski et al., 2014; Peres et al., 2019).

Several studies focused on the use of climate models to simulate future climate scenarios for hydrological analyses, have shown that changes in temperature and precipitation vary in space depending on the future climate scenario, type, and resolution of the models as well as on spatial heterogeneity of climatic features. This is particularly evident in the Mediterranean region, where, for instance, precipitation is partially controlled by orography, shows strong seasonality and large inter-annual fluctuations, and is characterized by the occurrence of particularly intense extreme events, such as prolonged droughts and high-intensity storms leading to floods (Bonaccorso et al., 2013, 2015a, b; Llasat et al., 2016; Senatore et al., 2020).

Recently, there has been a growing interest in the implementation of RCMs derived by dynamical downscaling of GCM outputs for climate change impact studies at small spatial scales. These are high-resolution models able to provide a more realistic representation of important surface heterogeneities (such as topography, coastlines, and land surface characteristics) and mesoscale atmospheric processes.

The Coordinated Regional Climate Downscaling Experiment (CORDEX) initiative is the first international programme providing a common framework to simulate both historical and future climate at the regional level, under different representative concentration pathways (RCPs; van Vuuren et al., 2011), and over different domains which cover all the land areas. More specifically, it provides climate data simulated by an ensemble of RCMs developed by several research centres all over the world that are forced by GCMs from the Coupled Model Intercomparison Project phase 5 (CMIP5; Taylor et al., 2012). In the present study, we refer to the CORDEX domain centred on the Euro-Mediterranean area, known as EURO-CORDEX (Jacob et al., 2014; http://www.euro-cordex.net, last access: 6 November 2020). In particular, EURO-CORDEX provides simulations for a historic reference period (baseline) and future projections up to 2100, with a 12.5 km grid resolution, available for four RCPs defined at the international level within CMIP5.

The reliability of individual RCMs in representing climate effects on the hydrological cycle depends on the quality of historical simulations and must be evaluated before using their output for impact assessment. Assessing RCM performance is essential to either select single models for further applications (e.g. Senatore et al., 2011; Peres et al., 2017; Smiatek and Kunstmann, 2019) or properly weight individual RCMs in multi-model ensembles to predict future impacts of climate change on hydrological processes (e.g. Christensen et al., 2010; Coppola et al., 2010). Table 1 provides a broad, although not thorough, list of inter-comparison studies within the CORDEX framework available in the literature. Overall, these studies show that CORDEX RCMs can reproduce the most important climatic features at regional scales, but important biases remain, especially regarding precipitation or climate extremes. As reported by Kotlarski et al. (2014) and references therein, model biases may depend on the analysed region, choices in model configuration, internal variability, and uncertainties of the observational reference data themselves (Gampe et al., 2019). Concerning the latter, a common approach in evaluation exercises consists of comparing models' simulations to observational gridded datasets from remote-sensing or model-derived reanalysis products available at global or continental spatial scales.

In general, statistical measures, such as bias, root mean square error, correlation, and trend analysis, are used to quantify model performance. Regardless of the specific methods used to assess the differences between simulated and observed data, one of the main limitations in this approach is that the considered spatial resolution is too coarse for reliable climate change impact studies at relevant hydrological scales, especially in areas of complex topography. From this point of view, large-scale observational gridded datasets are of poor applicability since they are built upon low-density hydro-meteorological networks.

In principle, more accurate evaluations can be achieved when they rely on gridded reference datasets that are obtained by spatial interpolation of point measurements onto a regular grid. To this end, two main prerequisites are that data coverage well reflects the topography, and variables with limited spatio-temporal climatic variability are investigated (Wagner et al., 2007). For example, Mascaro et al. (2018) compared the skill of several EURO-CORDEX RCMs at ~ 50 and 12 km grid spatial resolution in reproducing annual and seasonal precipitation regimes and trends in Sardinia (Italy) against a dense network of rain gauges with long-term records. Their analysis revealed that, although the simulated spatial patterns of annual and seasonal means are well correlated with the observations, positive and negative biases up to $\pm 60\,\%$ in the simulation of annual mean and inter-annual variability are detected. Furthermore, the majority of RCMs underestimate winter and overestimate summer precipitation. To the best of our knowledge, the available studies do not present an analysis on the quality by which drought event characteristics are reproduced by climate models.

In this study, we present an enhanced analysis over a different Mediterranean area with complex topography, namely the Sicily and Calabria regions (southern Italy). In particular, after investigating the ability of the EURO-CORDEX models

Table 1. Inter-comparison studies of RCM performances within the CORDEX framework.

References	Models	Variables	Region	Main conclusions
Schmidli et al. (2007)	Six statistical downscaling models (SDMs) and three RCMs	Daily precipitation	European Alps	SDMs and RCMs tend to have similar biases but differ with respect to inter-annual variations, with SDMs strongly underestimating the magnitude of the year-to-year variations, mainly in winter. RCMs indicate a strong trend toward drier conditions including longer periods of drought. The SDMs, on the other hand, show mostly non-significant or even opposite changes.
Endris et al. (2013)	10 RCMs from CORDEX Africa domain	Seasonal and annual precipitation	Eastern Africa and three subregions	RCMs reasonably simulate the main features of the precipitation climatology. However significant biases are detected in individual models depending on subregion and season. The ensemble mean has better agreement with observation than individual models.
Kotlarski et al. (2014)	Nine EURO-CORDEX RCMs	Spatio-temporal patterns of the European climate	Europe	The analysis confirms the ability of RCMs to capture the basic features of the European climate. Seasonally and regionally averaged temperature biases are mostly smaller than 1.5 °C, while precipitation biases are typically located in the ±40 % range.
Meque and Abiodun (2015)	10 RCMs from CORDEX Africa domain	Link between El Niño–Southern Oscillation (ENSO) and southern African droughts expressed by the Standardized Precipitation and Evapotranspiration Index (SPEI)	Southern Africa	ARPEGE model shows the best simulation, while CRCM shows the worst.
Mascaro et al. (2015)	Six RCMs driven by 10 GCMs from CORDEX Africa domain	Properties of the hydrological cycle	Niger River basin (West Africa)	Most RCMs overestimate (order of +10 % to +400 %, depending on model and sub-basin) the mean annual difference between precipitation (P) and evaporation (E).
Wu et al. (2016)	Four RCMs from the RMIP project and their regional multi-model ensemble and their driving GCM ECHAM5	Summer extreme precipitation	East Asia	All models can adequately reproduce the spatial distribution of extremely heavy precipitation. However, they do not perform well in simulating summer consecutive dry days. The ensemble average of multi-RCMs substantially improves model capability to simulate summer precipitation in both total and extreme categories when compared to each individual RCM.
Park et al. (2016)	Five RCMs form the CORDEX East Asia domain	Climatology of summer extremes (seasonal maxima of daily mean temperature and precipitation)	East Asia	RCMs show systematic bias patterns in both seasonal means and extremes. The models simulate temperature means more accurately compared to extremes because of the higher spatial correlation, whereas precipitation extremes are simulated better than their means because of the higher spatial variability.
Smiatek et al. (2016)	13 EURO-CORDEX RCMs	Mean temperature and precipitation, frequency distribution of precipitation intensity, maximum number of consecutive dry days	Greater Alpine Region (GAR)	Though the models reproduce spatial seasonal precipitation patterns, the seasonal mean temperature is underestimated (from −0.8 to −1.9 °C), and mean precipitation is overestimated (from +14.8 % in summer to +41.5 % in winter). Larger errors are found for further statistics and various GAR subregions.
Diasso and Abiodun (2017)	10 RCMs from CORDEX Africa domain	Drought characteristics evaluated through four principal components of the SPEI	West Africa	Only two models (REMO and CNRM) reproduce all the four drought modes. REMO and WRF give the best simulation of the seasonal variation in the drought mode over the Sahel in March–May and June–August seasons, while CNRM gives the best simulation of seasonal variation in the drought pattern over the savanna.
Um et al. (2017)	Four RCMs from CORDEX East Asia domain, their ensemble mean, and a driving GCM	Drought characteristics based on the SPEI	East Asia	Drought severity diverges markedly among the RCMs. Estimates of drought spatial extent are generally accurate in wet regions but inaccurate in dry regions. In general, the spatial extents of the droughts diverge among the RCMs, and the models fail to accurately capture droughts with large spatial scales.

Table 1. Continued.

References	Models	Variables	Region	Main conclusions
Foley and Kelman (2018)	Seven EURO-CORDEX RCMs and five driving GCMs	Several precipitation indices (accumulated precipitation amount, mean daily precipitation amount, max 1 and 5 d precipitation amounts, simple daily intensity, number of heavy and very heavy precipitation days)	Scottish islands	While no models perform skilfully across all the metrics studied, some models capture aspects of the precipitation climate at each location particularly well.
Adeniyi and Dilau (2018)	10 RCMs from CORDEX Africa domain	Precipitation, temperature, and drought	West Africa	ARPEGE has the highest skill at the Guinea coast, while PRECIS is the most skilful over the savanna and RCA over the Sahel.
Senatore et al. (2019)	Eight RCMs from CORDEX South Asia domain	Annual and seasonal precipitation and temperature	Iran and six subregions	No model is significantly better than others for every season and zone. Some enhancements are obtained by a weighting approach to take into account useful information from every RCM in the subzones. More reliable models show a strong precipitation decrease.
Di Virgilio et al. (2019)	Six RCMs from CORDEX Australasia domain	Near-surface max and min temperature and precipitation at annual, seasonal, and daily timescales	Australia	All RCMs showed widespread, statistically significant cold biases in maximum temperature and overestimated precipitation, especially over Australia's populous eastern seaboard.

to simulate the annual and seasonal temperature and precipitation regime, we analysed the skill in reproducing drought event characteristics identified through the run method (Yevjevich, 1967). Within the drought analysis, we also investigated the return period of drought events of fixed duration at both the annual and seasonal scales. In this case, given the limited number of droughts in a 30-year-long time series, an analytical framework was applied that allows the computation of the return period based on reasonable assumptions of the probabilistic structure of annual and seasonal precipitation (Bonaccorso et al., 2003; Cancelliere and Salas, 2004). Furthermore, we analysed model skills at a subregional level. To this aim, we proposed the use of principal component analysis (PCA) for delimitation of climatically homogeneous areas. The ability of climate models to reproduce observed precipitation, temperature, and drought features was analysed both per single characteristic and per multiple characteristics (e.g. precipitation and temperature together) by introducing a specific ranking criterion.

A total of 19 coupled GCM and RCM simulations within the EURO-CORDEX framework were evaluated against a high-density and high-quality monitoring-station-based reference dataset. Monthly temperature and precipitation records were retrieved by two monitoring networks, operated by the former Regional Hydrographic Services, whose density is significantly higher than observational datasets available at the European scale, such as E-OBS (Haylock et al., 2008) or CRU-TS (Harris et al., 2014), allowing for a more accurate evaluation of the models.

2 Study area and datasets

Our analyses were focused on the Calabria and Sicily regions in southern Italy, which, respectively, have an extension of 15 080 and 25 460 km^2, for a total area of 40 540 km^2 (Fig. 1a). Climate is of the Mediterranean type, with hot and dry summers and moderately cold winters with peak monthly precipitation occurring mostly in late autumn and winter. About 75 % of the total precipitation in the study area occurs from October to March because of cyclonic storms. These climate features make the area particularly prone to droughts, with the most recent severe episode occurring in 2017 (Rossi and Benedini, 2020). Climate features are also highly variable in space due to a rather complex orography. In particular, the mountain chains close to the coast enhance intense orographic precipitation and lead to relatively cold temperatures at the highest altitudes.

2.1 Observed data

Within the EURO-CORDEX control period (1951–2005), the comparison with observations was performed in the period from 1971 to 2000. These three decades had the greatest availability of historical series of precipitation and temperature recorded by the regional monitoring networks of both Calabria and Sicily, managed by the Multirisk Operational Centre of Calabria region (ArpaCal) and the Water Observatory of the Sicily region (WOS), respectively. Specifically, 84 thermometers (43 in Sicily and 41 in Calabria and near the regional borders) and 335 rain gauges (173 in Sicily and 162 in Calabria and near the regional borders) were used (Fig. 1a). Details on the monitoring network are given in the Supplement to this paper.

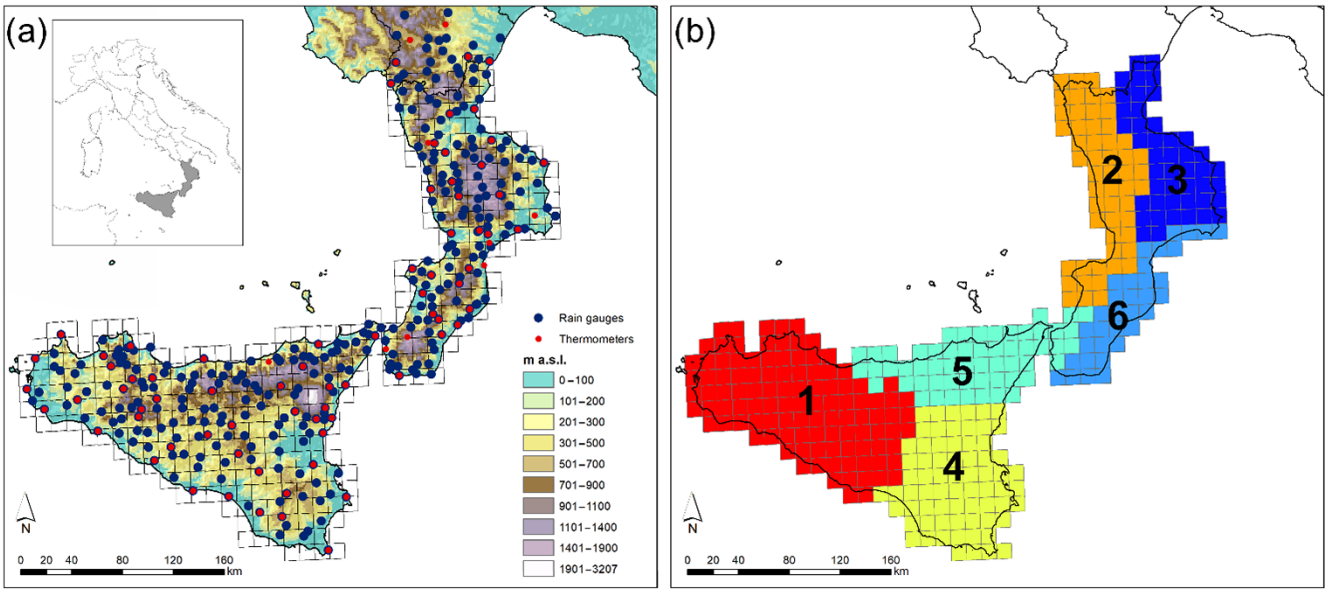

Figure 1. **(a)** Study area (Calabria is the southernmost peninsula of Italy, and Sicily is the neighbouring island) with the locations of the gauges of the high-density observational network and the CORDEX reference grid; **(b)** the six homogeneous zones identified through PCA.

The corresponding data were retrieved by the WOS (http://www.acq.isprambiente.it/annalipdf/, last access: 6 November 2020) and the ArpaCal (http://www.cfdcalabria.it, last access: 6 November 2020) websites. Observations were enough widespread to represent the quite heterogeneous features of the study area. The temperature stations were located between 2 and 1295 m a.s.l., with annual average values ranging from 9.2 to 20.6 °C (mean value $= 16.2 \pm 2.4$ °C), while the rain gauge elevations varied from 1 to 1369 m a.s.l., with annual accumulated values ranging from 373 to 1736 mm (mean value $= 812 \pm 287$ mm).

2.2 Climate models

Monthly precipitation and monthly mean air temperature data from the EURO-CORDEX CMIP5 simulations (Jacob et al., 2014; https://www.euro-cordex.net/ last access: 6 November 2020) were retrieved from the nodes of the Earth System Grid Federation (ESGF; e.g. https://esgf.llnl.gov, last access: 6 November 2020).

We analysed the data at the finest resolution, 0.11° (∼ 12.5 km; EUR-11) and considered the period 1971–2000 as a baseline. In particular, the combination of six GCMs (Table 2) and eight RCMs (Table 3), leading to 17 datasets, reported in Table 4, were collected for the study. Moreover, for two GCM–RCM combinations, two versions were available from the ESGF portal. Therefore, an overall ensemble of 19 combined models (CMs) was analysed. The ensemble mean of the 19 CMs was also evaluated. Even if the CMs have the same spatial resolution, each one is distributed on a specific grid (with slightly different origin and orientation of the axis). Therefore, the various datasets were resampled on the grid of the ECE-HIRH CM (Table 4), which is shown in Fig. 1a.

We choose EUR-11 rather than EUR-44 simulations as several studies (Torma et al., 2015; Prein et al., 2016) have found that generally higher-resolution CORDEX RCMs have better skills in simulating seasonal precipitation in regions with complex terrain.

3 Methodology

3.1 Data processing and PCA

To allow the comparison between the spatially distributed RCM data and site-specific observations, the latter were spatially interpolated using the CORDEX 0.11° grid as reference (Fig. 1a). In this way, month by month, each cell of the CORDEX grid could be associated with a single temperature or precipitation value derived from the observation network. Specifically, concerning temperature, an inverse distance weighted (IDW) interpolation was applied to the residuals of the values obtained using a regression model with the altitude. For precipitation, whose measurement network is much denser, a simple IDW interpolation was performed. As shown in Fig. 1a, the CORDEX grid cells which are not covered by any rain gauge are relatively few (less than 30 %), and, except one case, the distance of the closest rain gauge to every grid cell is always less than 10 km.

The precipitation patterns obtained by the interpolation procedure were analysed, adopting a methodology based on the principal component analysis (PCA) to distinguish zones with rather independent climatic variability within the area

Table 2. List of GCMs, together with the abbreviations used in this paper, included at least once in the EURO-CORDEX ensemble.

Model name	Abbreviation	Reference	Institution
CNRM-CERFACS-CNRM-CM5	CM5	Voldoire et al. (2013)	Centre National de Recherches Météorologiques
ICHEC-EC-EARTH	ECE	Hazeleger et al. (2010)	Irish Centre for High-End Computing EC-Earth Consortium, Europe
IPSL-IPSL-CM5A-MR	IPS	Dufresne et al. (2013)	Institut Pierre Simon Laplace
MOHC-HadGEM2-ES	Had	Collins et al. (2011)	Met Office Hadley Centre
MPI-M-MPI-ESM-LR	MPI	Giorgetta et al. (2013)	Max Planck Institute for Meteorology
NCC-NorESM1-M	Nor	Bentsen et al. (2013), Iversen et al. (2013)	Norwegian Earth System Model

Table 3. List of RCMs, together with the abbreviations used in this paper, included at least once in the EURO-CORDEX ensemble.

Model name	Abbreviation	Reference	Institution
CNRM-ALADIN53	ALAD	Colin et al. (2010)	Météo-France/Centre National de Recherches Météorologiques
RMIB-UGent-ALARO-0	ALAR	De Troch et al. (2013)	Royal Meteorological Institute of Belgium and Ghent University
CLMcom-CCLM4-8-17	CCLM	Baldauf et al. (2011), Rockel et al. (2008)	Climate Limited-area Modelling Community (CLM-Community)
DMI-HIRHAM5	HIRH	Christensen et al. (2007)	Danish Meteorological Institute
KNMI-RACMO22E	RACM	van Meijgaard et al. (2008)	Royal Netherlands Meteorological Institute, De Bilt, the Netherlands
SMHI-RCA4	RCA4	Strandberg et al. (2014)	Swedish Meteorological and Hydrological Institute, Rossby Centre
MPI-CSC-REMO2009	REMO	Teichmann et al. (2013)	Helmholtz-Zentrum Geesthacht, Climate Service Center, Max Planck Institute for Meteorology
IPSL-INERIS-WRF331F	WRF3	–	Institut Pierre-Simon Laplace and French National Institute for Industrial Environment and Risks (Ineris)

under investigation. PCA is a well-known statistical tool used to transform an original set of intercorrelated variables into a reduced number of new linearly uncorrelated ones explaining most of the total variance (Rencher, 1998). The latter, derived as linear combinations of the original variables, are the principal components (PCs), while the coefficients of the linear combinations are the loadings, which in turn represent the weight of the original variables in the PCs. From a procedural standpoint, PCA consists of solving an eigenvalue–eigenvector problem applied to the covariance matrix. The eigenvectors, properly normalized, are the loadings of the principal components, while the eigenvalues provide a measure of the total variance explained by each loading (Bordi and Sutera, 2001, and references therein). Under this decomposition, the loadings represent the correlation between the associated PCs and observed time series. Mapping the loading patterns of each PC among those selected, based on the percentage of the total explained variance of the process, largely allows the identification of independent climatic areas within the study region. Moreover, it may be useful to apply a rotation operation to the eigenvectors so that the corresponding loadings are more spatially localized. In other words, the rotation leads to loadings with a high correlation with a smaller set of spatial variables and a low correlation with the remaining variables. Here, only orthogonal rotations were considered, computed by the varimax algorithm in MATLAB® (2016). Clearly, each rotated pattern will not explain the same variance of the unrotated one, although the total variance explained remains unchanged.

In the present study, the first nine rotated PCs at both the annual and seasonal (December–February, DJF; March–May, MAM; June–August, JJA; September–November, SON) scales were investigated. Regardless of the considered period, the selected PCs always explain more than 78 % of the total variance, with a maximum of 85 % in the winter season (DJF). The loading patterns of these rotated PCs were mapped for each considered period to identify climatically homogeneous regions. Homogeneous subregions were detected at the annual scale and in autumn and winter, whereas a confusing picture arose in spring and summer. Furthermore, since about 75 % of the total annual rainfall of the case study area occurs between autumn and winter (as a re-

sult of cyclonic storms), the climatically homogeneous subregions identified at the annual scale approximately overlap with those identified in SON and DJF. Isolated grid cells showing a different PC correspondence with respect to the surrounding cells were manually corrected to simplify the delimitation of the homogeneous subregions. This approach led to dividing the whole area into six climatically homogenous zones, three for Sicily and three for Calabria (Fig. 1b), for which separate performance assessments were carried out. Concerning the Sicily region, the three identified subregions roughly coincide with the ones detected by Bonaccorso et al. (2003), who investigated the spatial variability of droughts in the Sicily region based on Standardized Precipitation Index (SPI) series computed on monthly precipitation observed in traditional rain gauges and on NCEP/NCAR reanalysis data from 1926 to 1996. In particular, three distinct areas, namely north-eastern (identified in the PCA as Zone 5), south-central-eastern (Zone 4), and central-western (Zone 1), were identified. In Calabria, three main zones were also determined, namely north-western (Zone 2), north-eastern (Zone 3), and south-eastern (Zone 6), broadly corresponding to climatically homogenous areas found in previous studies (e.g. Versace et al., 1989). Interestingly, the south-western tip of Calabria is identified as a part of a broader area (Zone 5) extending over the north-eastern Sicily.

3.2 Performance metrics and model ranking

The CMs were evaluated based on their performances in capturing specific properties, namely the inter-annual and seasonal variability of precipitation, temperature, and drought characteristics. Such properties were expressed based on some relevant statistics.

Let $X(j)$ and $X_\tau(j)$ be the variable under investigation (precipitation or mean temperature) at grid cell j at the annual and seasonal scale, respectively. For precipitation and mean air temperature, the following statistics were derived for each CM and cell in the area of interest:

- seasonal mean $\mu_m(X_\tau(j)) = \frac{\sum_{v=1}^{N} x_{v,\tau,m}(j)}{N}$,

  where $x_{v,\tau m}(j)$ is the value of the variable in season τ ($\tau = 1, 2, 3, 4$) and year v ($v = 1, 2, \ldots N$) produced by the mth CM ($m = 1, 2, \ldots M$) at grid cell j. Seasons are DJF, MAM, JJA, and SON;

- seasonal standard deviation $\sigma_m(X_\tau(j)) = \sqrt{\frac{\sum_{v=1}^{N}\left(x_{v,\tau,m}(j)-\mu_m(X_\tau(j))\right)^2}{N-1}}$;

- annual mean $\mu_m(X(j)) = \frac{\sum_{v=1}^{N} X_{v,m}(j)}{N}$;

  where $x_{v,m}$ is the value of the variable at year v ($v = 1, 2, \ldots N$) produced by the mth CM at the grid cell j;

- annual standard deviation $\sigma_m(X(j)) = \sqrt{\frac{\sum_{v=1}^{N}\left(x_{v,m}(j)-\mu_m(X(j))\right)^2}{N-1}}$.

Drought events were identified on both annual and seasonal (DJF, MAM, JJA, SON) precipitation values simulated for the period 1971–2000 according to the theory of runs (Yevjevich, 1967). In particular, drought events were selected as the periods during which consecutive annual or seasonal values of precipitation did not exceed a given threshold, here assumed equal to the long-term means of annual and seasonal data (i.e. one threshold for each season). Once drought events were identified, the corresponding drought characteristics in each cell were determined. In particular, the following statistics for drought characteristics are considered hereafter to assess the models' performance.

- Maximum drought duration $L_{\max}$: maximum length of periods with consecutive annual precipitation values below the threshold;
- Maximum drought accumulated deficit $D_{\max}$: maximum of the sums of the differences between the threshold and the precipitation values along with the drought duration;
- Maximum drought intensity $I_{\max}$: maximum of the ratio between drought accumulated deficit and duration;
- Return period of drought events of fixed duration (at both annual and seasonal scales).

Concerning the return period of drought events, let E be a critical drought (e.g. a drought with duration L equal to a fixed value). Assuming independence between consecutive drought events, the return period of drought events E can be expressed as (Gonzales and Valdes, 2003; Cancelliere and Salas, 2004, 2010; Bonaccorso et al., 2012)

$$T_E = \frac{E[L] + E[L_n]}{P[E]}, \tag{1}$$

where $E[L]$ is the expected value of drought duration L, $E[L_n]$ is the expected value of the non-drought duration L_n, and $P[E]$ is the probability of occurrence of a critical drought E, which can be determined once the probability distribution function of the event E is known.

Regarding the probability distribution of drought duration, let us consider a stochastic hydrological variable denoted as $X_{v,\tau}$, where v represents the year, and τ represents the season. According to the theory of runs, drought duration L is the number of consecutive time intervals (seasons) where $X_{v,\tau} \le x_{o,\tau}$ is preceded and followed by at least one season where $X_{v,\tau} > x_{o,\tau}$, where $x_{o,\tau}$ is a threshold level representing water demand. The original variable can be replaced by a Bernoulli variable $Y_{v,\tau}$ such that

$$\begin{cases} Y_{v,\tau} = 0 \text{ if } X_{v,t} \le x_{0,\tau} \text{ (deficit)} \\ Y_{v,\tau} = 1 \text{ if } X_{v,t} > x_{0,\tau} \text{ (surplus).} \end{cases} \tag{2}$$

Assuming that $Y_{v,\tau}$ is a lag-1 Markov stationary process, it can be shown (Sen, 1976; Cancelliere and Salas, 2004, 2010) that the probability distribution of drought duration L is geometric with parameter p_{01}:

$$f_L(l) = P[L = l] = (1 - p_{01})^{l-1} p_{01}. \quad (3)$$

The parameter p_{01} represents the transition probability from a deficit to a surplus, namely $p_{01} = \left[Y_{v,\tau} = 1 \middle| Y_{v,\tau-1} = 0\right]$.

Estimation of transition probabilities can be carried out following a non-parametric approach based on maximum likelihood, which leads to (Bonaccorso et al., 2012)

$$p_{01} = 1 - p_{00} = 1 - \frac{n_{00}}{n_{00} + n_{01}}, \quad (4)$$

where n_{00} is the number of observations $y_{v,\tau} = 0$, for which $y_{v,\tau-1} = 0,$, and n_{01} is the number of observations $y_{v,\tau} = 1$, for which $y_{v,\tau-1} = 0$.

For independent stationary series, the probability distribution of drought duration L is geometric with parameter $p_1 = P[Y_\tau = 1]$. The latter can be simply estimated by applying a frequency analysis on Y_τ.

Following previous studies (Bonaccorso et al., 2003; Cancelliere and Salas, 2004), the annual series were assumed independent stationary, whereas the seasonal series were assumed as lag-1 stationary Markov.

Models' skills in reproducing the inter-annual and seasonal variability of precipitation and mean air temperature variables were first assessed through

- box plots of the errors and percentage errors of the mean values in all the grid cells of the investigated areas, which allow the analysis of the spatial variability of the models' bias;
- Taylor diagrams (Taylor, 2001), which show three metrics at the same time, i.e.: coefficient of correlation, standard deviation, and centred root mean square error of the anomalies (i.e. the variables of interest minus the corresponding means). It is noteworthy that standard Taylor diagrams do not provide any information about first-order statistics (i.e. bias).

Later, to provide synthetic information about each CM starting from the various statistics computed for each property, a method based on Mascaro et al. (2018) was used. Specifically, for each property (i.e. seasonal and inter-annual variability of precipitation and mean temperature and drought characteristics), a single dimensionless error metric that combines multiple statistics characterizing that property was estimated. The error metric follows the equation

$$\varepsilon_m = \sqrt{\sum_{k=1}^{S} \left(\frac{\sum_{j=1}^{P} E_{k,m}(j)}{\sum_{m=1}^{M} \sum_{j=1}^{P} E_{k,m}(j)} \right)^2}, \quad (5)$$

where $E_{k,m}(j)$ represents an error metric between observed and simulated data of the statistics k $(k = 1, \ldots, S)$ at grid cell j $(j = 1, \ldots P$, where P is the total number of grid cells), whose sum over the whole area was divided by the sum of the error metrics of all models, therefore resulting in a dimensionless indicator for each statistic k of any property. Table 5 summarizes the statistics chosen for each property and describes how the corresponding errors were calculated.

Based on the values of the error metrics in Eq. (5), a ranking of the models, describing the skills in reproducing each property, was obtained. It should be specified that while, for the sake of brevity, the box plots and the Taylor diagrams illustrated in the next section refer to the whole study area, the ranking of the models for the mean air temperature, precipitation, and drought characteristics also refers to the six climatically homogenous zones identified through PCA. This analysis, indeed, can help to highlight whether some models are more suitable than others to simulate certain variables in a given zone.

4 Results

In this section, results are presented and discussed separately for temperature, precipitation, and drought characteristics. Results are differentiated for the following temporal and spatial aggregation scales: annual data, seasonal data, the whole case study region, and the six climatically homogenous areas identified via PCA.

4.1 Mean air temperature

4.1.1 Inter-annual variability

The observed and modelled means of the annual mean air temperature values in each of the grid cells within the study area were calculated and compared. More specifically, for each cell j, the error corresponding to the mth CM was computed as

$$E_{m,j} = \mu_m(T(j)) - \mu_0(T(j)), \quad (6)$$

where $T(j)$ is the mean annual temperature at cell j, whereas $\mu_m(\cdot)$ and $\mu_0(\cdot)$ are the modelled and observed means, respectively. For each model, the distribution of the errors computed for all the grid cells of the study area based on Eq. (6) is represented in the form of box plots in Fig. 2a. In particular, the central line represents the median value, and the box is delimited by the first and the third quartile. The width of the box corresponds to the inter-quartile range (IQR), a well-known measure of dispersion. Values outside the whiskers beyond at least 1.5 times the IQR from the box can be assumed as outliers.

The overall tendency of the models is to underestimate temperatures as the medians are negative. Errors are predominantly between the values -5 and $-1\,^{\circ}\mathrm{C}$, thus implying that the models underestimate up to $5\,^{\circ}\mathrm{C}$. The CMs that produce the most extreme negative errors are the ECE-RACM,

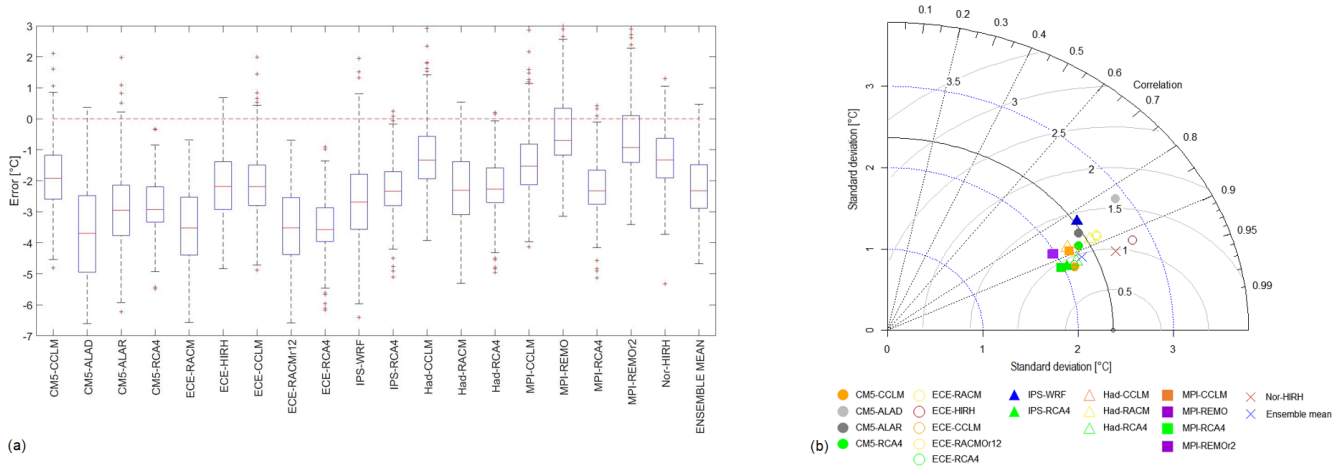

Figure 2. **(a)** Box plots representing the frequency distribution of RCM errors in mean annual temperature for the whole study area. **(b)** Taylor diagram comparing model performances in reproducing the inter-annual variability of mean temperature for the whole study area.

ECE-RACMr12, and CM5-ALAD, with the latter showing the broader IQR (e.g. the highest spatial variability of the errors) and the greatest median error. All the CMs with RCA4 show the smallest IQR. The models with the smallest median error are MPI-REMO and MPI-REMOr2.

To extend the CM skill comparison to other statistics, the Taylor diagram for the annual mean air temperature values was developed (Fig. 2b). For the sake of simplicity, standard deviations of the CMs are indicated as σ hereinafter. The diagram allows the visualization of possible clusters of performances related to specific GCMs or RCMs among those considered. In the diagram, GCMs are indicated with different markers, while RCMs are indicated with different colours. The value corresponding to the observations is the dot on the x axis, whose standard deviation is marked through a continuous circular arc. In addition to every single model, the ensemble mean model result is reported in the diagram.

Figure 2b shows that the simulated means are well correlated with the observations, with values larger than 0.8 for all the considered models. Furthermore, the diagram seems to reveal that, on equal GCMs, RCMs play a significant role in determining the performance of the combinations. In general, for most of the models, the best performances are obtained when the RCM RCA4 is used. The only exception is CM5, performing better in combination with CCLM. The worst models are CM5-ALAD and IPS-WRF.

Finally, the ranking analysis described in Sect. 3.2 yields the results in Fig. 3. The lower the rank is, the lower the error metrics in Eq. (5) are and the better the model is. For better readability, ranking values are indicated through a chromatic scale, ranging from dark green (first-ranked model) to dark red (last-ranked model).

The best-performing models, in terms of ranking order for the whole study area, are MPI-CCLM, MPI-REMO, and Had-CCLM. ECE-RCA4 and CM5-CCLM are also good models, as highlighted by the Taylor diagrams. Figure 3 also shows rankings for each of the six homogeneous areas. As can be observed, based on the range of colours in each row, MPI-CCLM and MPI-REMO provide the best performance for almost all the zones.

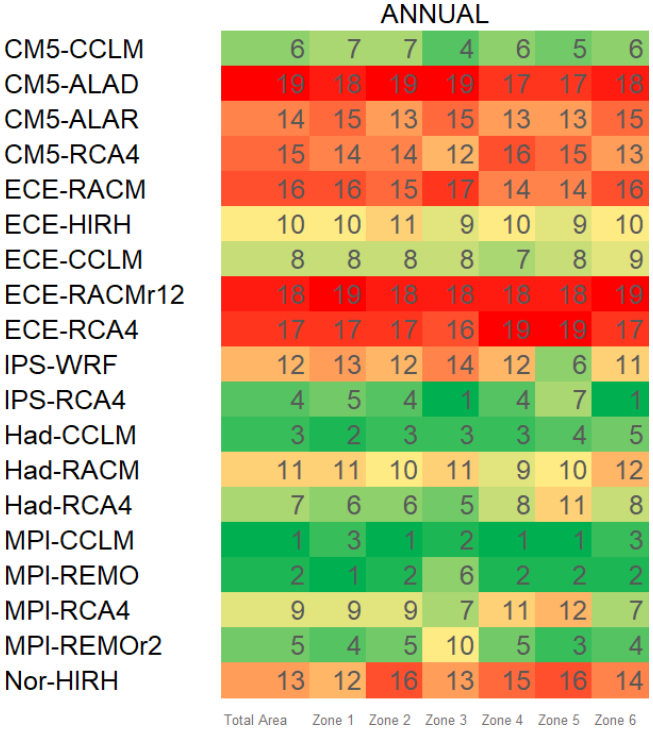

Figure 3. RCM ranking with respect to inter-annual variability of mean temperature, for the entire area and the climatically homogenous zones.

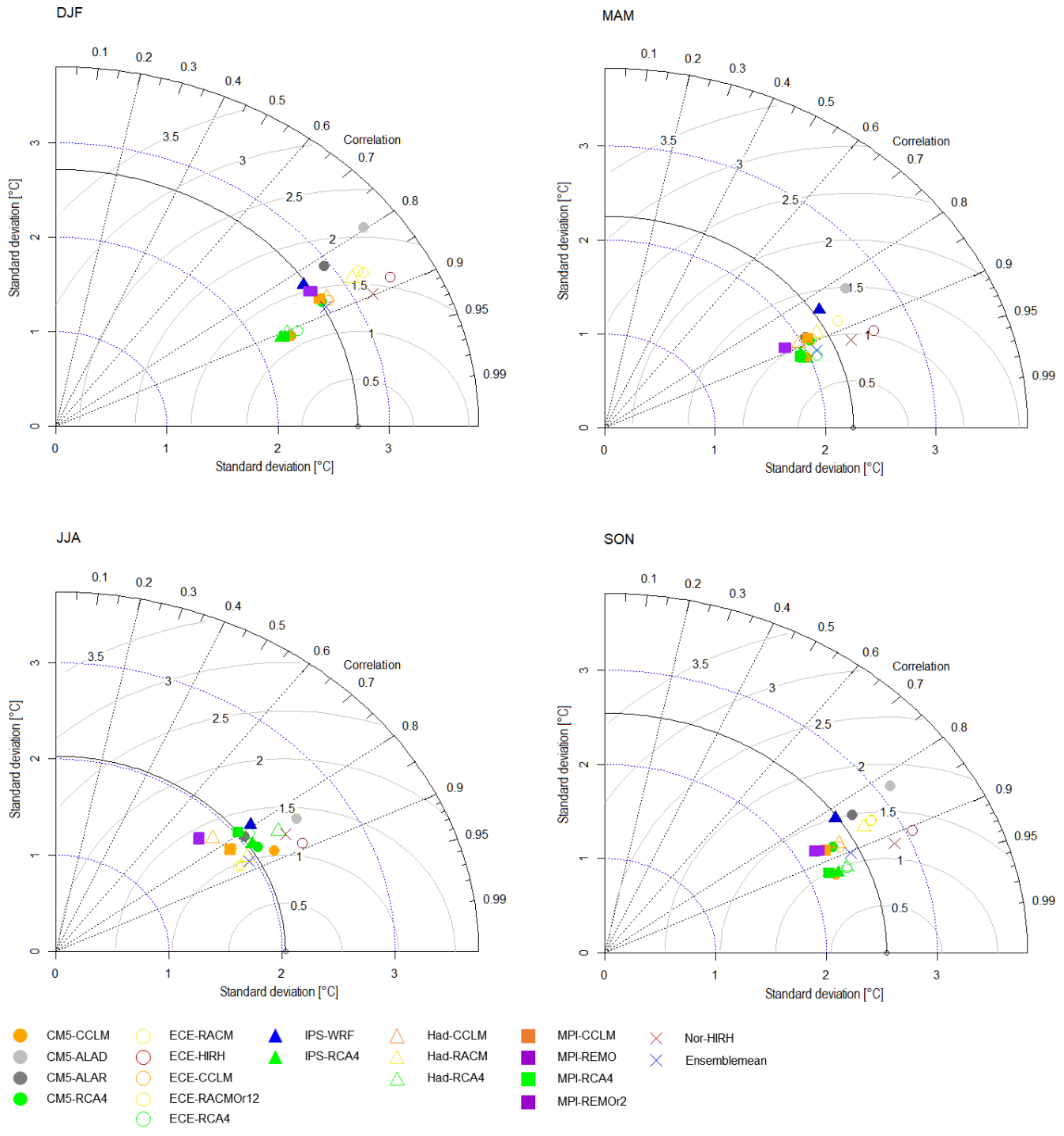

Figure 4. Taylor diagram comparing model performances in reproducing the seasonal variability of mean temperature for the whole study area.

Indeed, some differences exist for Zones 3 and 6 (north and south-eastern Calabria), whose best CM is IPS-RCA4. Overall, results show that the worst model is CM5-ALAD for entity and dispersion of errors, lower correlations, higher RMSE, and greater departure from the standard deviation of the observed values, both for the whole study area and individual zones. ECE-RACM, ECE-RACMr12, and ECE-RCA4 also show bad performance (the latter mainly because of its relatively strong bias).

Table 4. List and abbreviations of climate models (GCM–RCM combinations) included at least once in the EURO-CORDEX ensemble. The asterisk (*) means that two versions of the GCM–RCM combination are available. The first row lists the GCMs, while the first column lists the RCMs.

	CNRM-CERFACS-CNRM-CM5	ICHEC-EC-EARTH	IPSL-IPSL-CM5A-MR	MOHC-HadGEM2-ES	MPI-M-MPI-ESM-LR	NCC-NorESM1-M
CNRM-ALADIN53	CM5-ALAD	–	–	–	–	–
RMIB-UGent-ALARO-0	CM5-ALAR	–	–	–	–	–
CLMcom-CCLM4-8-17	CM5-CCLM	ECE-CCLM	–	Had-CCLM	MPI-CCLM	–
DMI-HIRHAM5	–	ECE-HIRH	–	–	–	Nor-HIRH
KNMI-RACMO22E	–	ECE-RACM*	–	Had-RACM	–	–
SMHI-RCA4	CM5-RCA4	ECE-RCA4	IPS-RCA4	Had-RCA4	MPI-RCA4	–
MPI-CSC-REMO2009	–	–	–	–	MPI-REMO*	–
IPSL-INERIS-WRF331F	–	–	IPS-WRF	–	–	–

4.1.2 Seasonal variability

For the sake of brevity, the box plots related to the seasonal variability of mean air temperature are not shown since they provide similar results to the case of annual variability.

Figure 4 shows the Taylor diagrams obtained from the analysis of the individual seasons. CM5-ALAD and IPS-WRF (and, to a slightly lesser extent, CM5-ALAR) appear as the worst models regardless of the season, although in summer (JJA) the worst-performing models are MPI-REMO and MPI-REMOr2. Summer is also the season with the (slightly) lowest values of correlation coefficients.

Regarding the best models, in general, all the combinations with RCA4 and the CM5-CCLM work better, as for the analysis of inter-annual variability. However, in summer, better performances are obtained with ECE-RACM and ECE-RACMr12.

Figure 5 represents the rankings of the models for the individual seasons and all the study areas, namely the whole case study and the six zones. There is a certain correspondence of the worst-performing models between Figs. 4 and 5. Nonetheless, differently from the results in Fig. 3, models' performances may change significantly from season to season and, in the same season, from zone to zone. The best models for most of the zones are ECE-HIRH in winter (DJF), ECE-CCLM in spring (MAM), IPS-RCA4 in summer (JJA), and MPI-REMOr2 in autumn (SON). It is worth highlighting that the latter provides the best performances also for Zones 2 and 4 in spring and Zones 5 and 6 in summer. Conversely, ECE-HIRH, which is the best model in winter, works poorly in summer and autumn. Zones 1 (western Sicily) and 2 (western Calabria) show a uniform behaviour in all seasons, with the only exception being spring, while Zones 5 (north-eastern Sicily) and 6 (south-eastern Calabria) show a uniform behaviour in all seasons but autumn. Besides, in summer and autumn, the best-performing models for Zones 1, 2, and 4 (south-eastern Sicily) are the same as for the whole study area. Zone 3 (north-eastern Calabria) behaves like Zone 4 in winter and like Zones 1, 5, and 6 in spring.

4.2 Precipitation

4.2.1 Inter-annual variability

Figure 6a shows box plots for the percentage errors in mean annual precipitation, namely

$$E_{m,j} = \frac{\mu_m(P(j)) - \mu_0(P(j))}{\mu_0(P(j))} \cdot 100, \tag{7}$$

where $P(j)$ is the total annual precipitation at the grid cell j.

In comparison to temperature, the errors are much larger as well as the differences between the various models. There is a general tendency for the models to underestimate the total annual precipitation, except for some models like IPS-WRF, which also shows the largest IQR. The median value of the

Table 5. Summary of the statistics involved in the ranking process. Statistics with subscript $_0$ refer to observed values.

Property	Statistics k	Error $E_{k,m}(j)$
Seasonal variability	Seasonal mean	$\lvert\mu_0(X\tau(j)) - \mu_m(X_\tau(j))\rvert$
	Seasonal standard deviation	$\lvert\sigma_0(X\tau(j)) - \sigma_m(X_\tau(j))\rvert$
Inter-annual variability	Annual mean	$\lvert\mu_0(X(j)) - \mu_m(X(j))\rvert$
	Annual standard deviation	$\lvert\sigma_0(X(j)) - \sigma_m(X(j))\rvert$
Drought characteristics	Maximum drought duration	$\lvert L_{\max,0}(j) - L_{\max,m}(j)\rvert$
	Maximum drought accumulated deficit	$\lvert D_{\max,0}(j) - D_{\max,m}(j)\rvert$
	Maximum drought intensity	$\lvert I_{\max,0}(j) - I_{\max,m}(j)\rvert$
	Return period	$\lvert T_{r,0}(j) - T_{r,m}(j)\rvert$

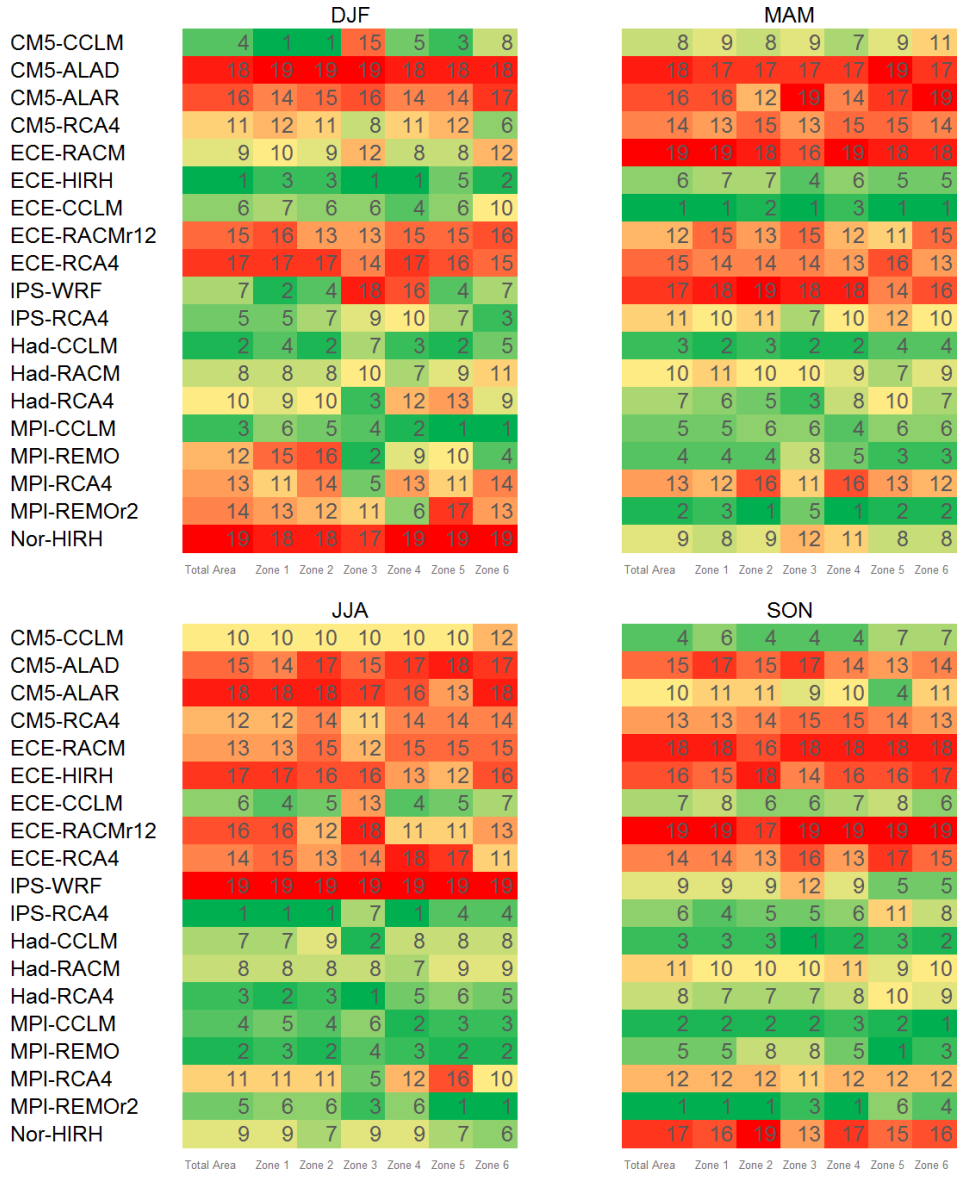

Figure 5. RCM ranking with respect to seasonal variability of mean temperature for the entire area and the climatically homogenous zones.

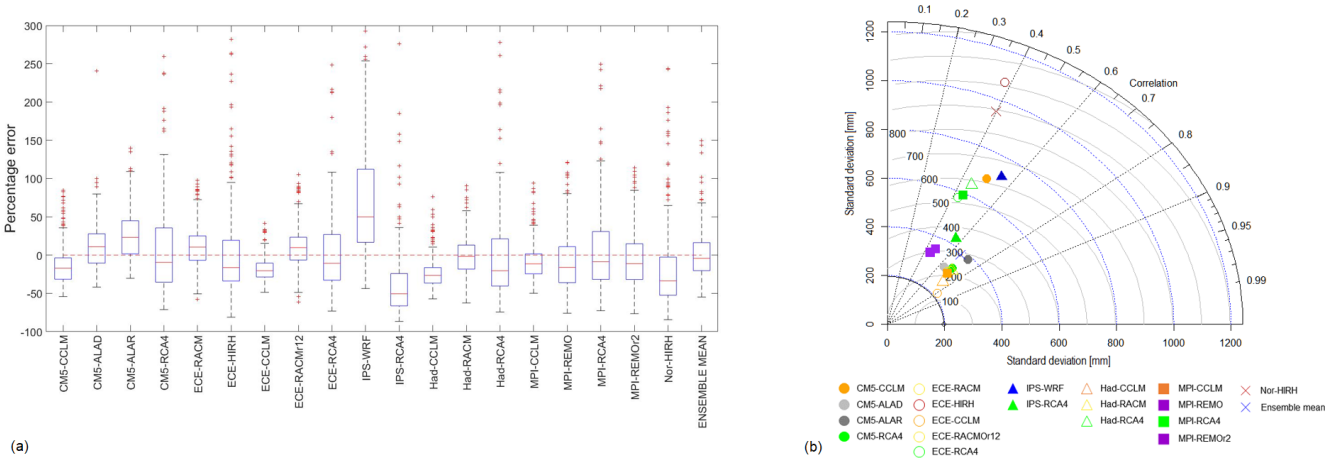

Figure 6. (a) As Fig. 2a but for annual precipitation. **(b)** As Fig. 2b but for annual precipitation.

relative errors for some models is less than 20 %; however, many models have a large dispersion with error values over 100 %. The CM with the highest positive error is IPS-WRF, while the ones with the highest negative errors are the IPS-RCA4 and Nor-HIRH models. The GCM–RCM combinations with the smallest IQR of errors are those using CCLM RCMs. The model with the smallest bias is Had-RACM.

The Taylor diagram in Fig. 6b confirms that the best combinations are those with CCLM RCMs. In particular, the best one seems to be ECE-CCLM. However, when used in combination with CM5, the corresponding model provides poor performance. The worst-performing models are ECE-HIRH and Nor-HIRH. The diagram confirms that precipitation is modelled with less accuracy than temperature as correlations are lower (< 0.8).

The application of the ranking criteria (see Fig. 7) suggests Had-RACM and ECE-CCLM as the best combinations for the entire area and most of the zones. Also, CM5-ALAD works well for the whole area and almost all the zones, except for Zone 4, where it ranks 11th. IPS-WRF, IPS-RCA4, Nor-HIR, and CM5-RCA4 are the worst models.

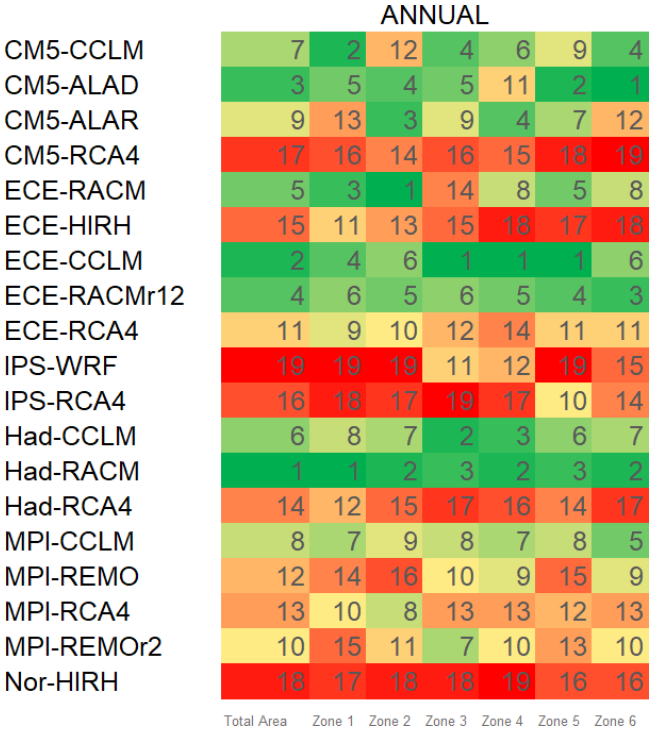

Figure 7. As Fig. 3 but for annual precipitation.

4.2.2 Seasonal variability

The seasonal variability analysis carried out on precipitation shows (Fig. 8) a lower error dispersion in the wet seasons (i.e. autumn and winter) with respect to summer. In summer, several models show broader IQRs, such as all the CM5 models and IPS-WRF, with the latter showing the largest median error. On the one hand, these outcomes depend on the poor performance of some models in reproducing the seasonal cycle and on the other hand are due to the fact that in the dry season, when rainfall is normally low, large errors may result even though the departure from the observed mean is relatively small. These results are consistent with those obtained by Giorgi and Lionello (2008) in a subdomain of the Mediterranean region and by Mascaro et al. (2018) for the Sardinia region.

The Taylor diagrams in Fig. 9 highlight that NOR-HIRH and ECE-HIRH are the worst models for all the seasons but summer, where the IPS-WRF is the worst-performing.

These indications are confirmed by the ranking results in Fig. 10. Concerning the best models, the following CMs perform the best in their respective seasons: ECE-RACMr12 in winter (DJF), ECE-CCLM in spring (MAM), MPI-REMOr2 in summer (JJA), MPI-CCLM and Had-RACM in autumn

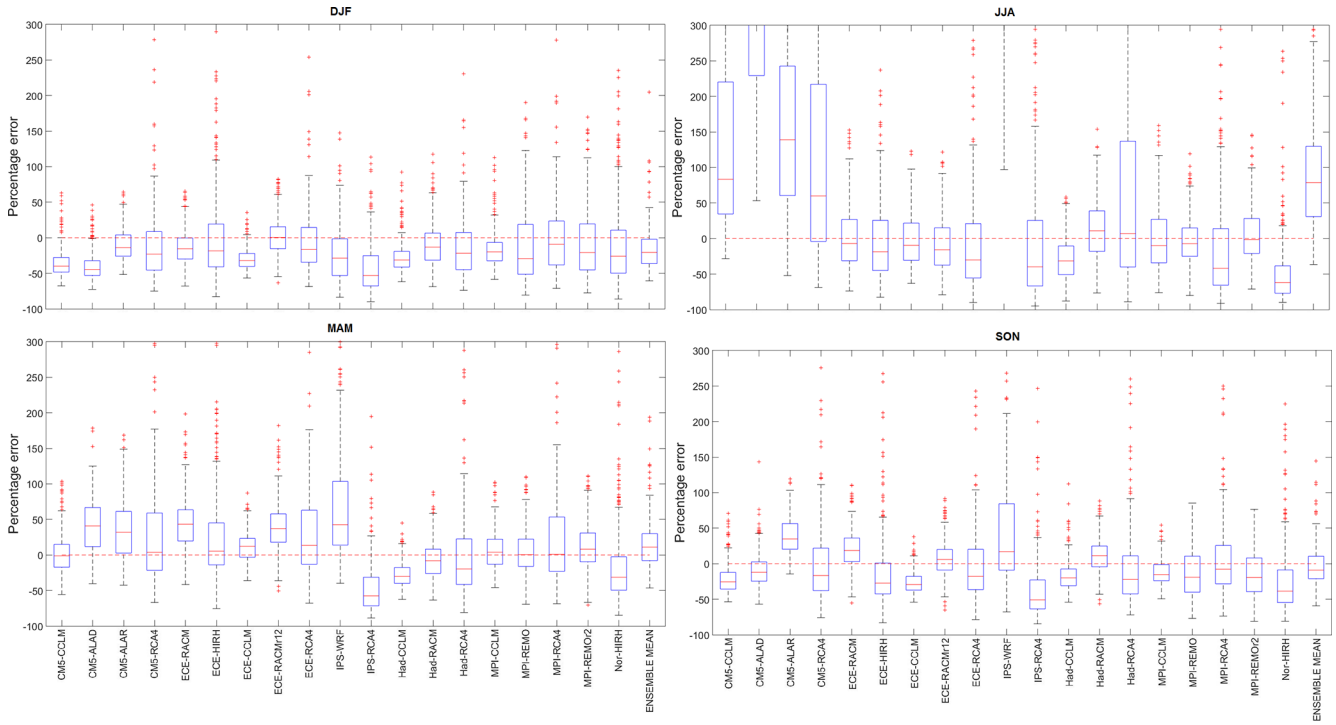

Figure 8. Box plots representing the frequency distribution of RCM percentage errors in seasonal precipitation for the whole study area.

(SON). It is worth highlighting that ECE-RACMr12 provides the best rank also for Zone 2 in autumn; ECE-CCLM is the best-performing also for Zone 6 in summer; MPI-CCLM provides the best performances also for Zone 1 in winter and Zone 4 in spring, and Had-RACM is the best model for Zone 2 in spring. For summer precipitation, MPI-REMOr2 is the best-performing CM also for Zones 1, 2, 3, and 4. As for the ranking of seasonal mean temperature, once again there is no uniform behaviour of the models between the different seasons and zones.

4.3 Drought characteristics

4.3.1 Annual scale

The models' performance in reproducing historical drought characteristics at both the annual and the seasonal scale was also tested. In particular, the following drought characteristics derived from the theory of runs were analysed: maximum duration (L_{max}), maximum accumulated deficit (D_{max}), and maximum intensity (I_{max}) and return period of drought duration.

With reference to the drought characteristics identified on annual precipitation, Fig. 11a, b, and c represent the box plots of the errors related to maximum drought duration, accumulated deficit, and intensity, respectively. In particular, for drought duration, the errors were computed through Eq. (6) by simply replacing T with L_{max}, whereas for maximum drought accumulated deficit and intensity, the percentage errors were calculated through Eq. (7) by replacing P first with D_{max} and then with I_{max}.

There is a slight tendency of some models to underestimate drought duration (Fig. 11a). Overall, the errors span from -3 to $+2$ years. The broadest IQR is associated with MPI-REMO, while some models, such as CM5-CCLM, CM5-ALAR, ECE-RACM, and Nor-HIRH, seem equally reliable.

The box plots obtained for D_{max} (Fig. 11b) show that the models may yield considerable errors, which can potentially be larger than those for annual precipitation as the accumulated deficit, given by the sum of precipitation deficits in a time interval lasting several years, can be affected by multiple errors. For some models, the IQRs are not larger than 50 %. The most reliable model is Had-CCLM, but comparable performances are given by models CM5-CCLM, CM5-ALAR, and ECE-CCLM, while the least dispersed is MPI-CCLM (for this model, however, the median error is larger than others). The least reliable is IPS-WRF, followed by CM5-RCA4 and MPI-REMOr2. In general, as can be seen from the box plots, this feature is underestimated. Concerning I_{max}, the results indicate Had-RACM as the best model and CM5-RCA4 as the worst, followed by IPS-WRF (Fig. 11c). Errors for this feature are less scattered than for accumulated deficit, and there is a general tendency for I_{max} to be underestimated by models.

Figure 12 shows box plots of the errors in the return period of drought events of duration L equal to 1, 3, 5, and 7 years,

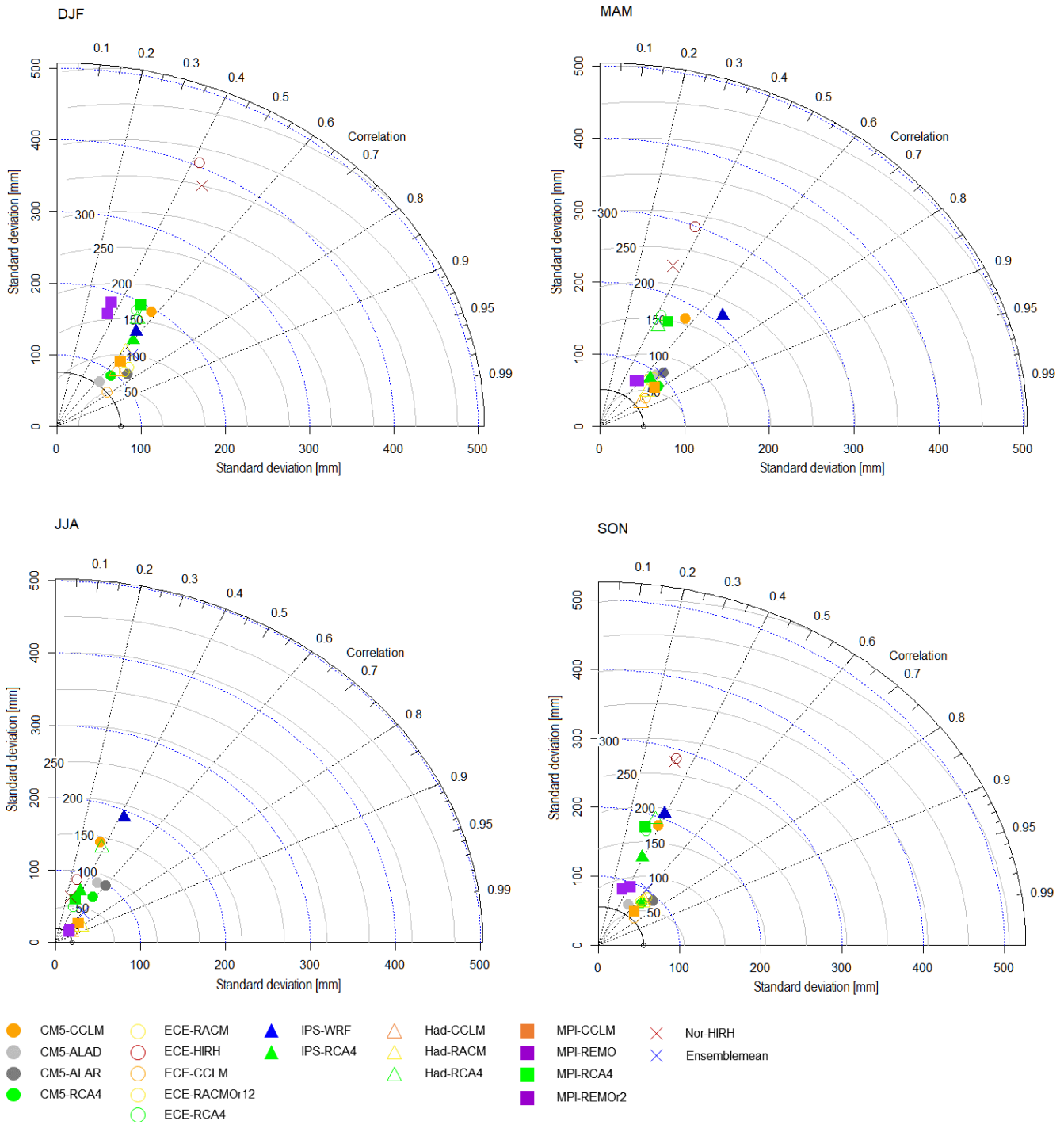

Figure 9. As Fig. 4 but for seasonal precipitation.

respectively. In particular, the error was calculated as

$$E_{m,j} = \mu_m\left(T_y\left(j\right)\right) - \mu_0\left(T_y\left(j\right)\right)\varepsilon_j = \mu_{\mathrm{m}}\left(X\left(j\right)\right) - \mu_0\left(X\left(j\right)\right), \tag{8}$$

where $T_y(j)$ is the return period of a drought event of fixed duration at the grid cell j.

As expected, for any given model, the error increases as the considered drought duration increases. However, regardless of the drought duration, there is no general tendency of the models towards overestimation or underestimation of the return periods. ECE-CCLM and Had-RACM are the models with the smallest IQR, with ECE-CCLM showing the lowest median error. Overall, the performance of the mod-

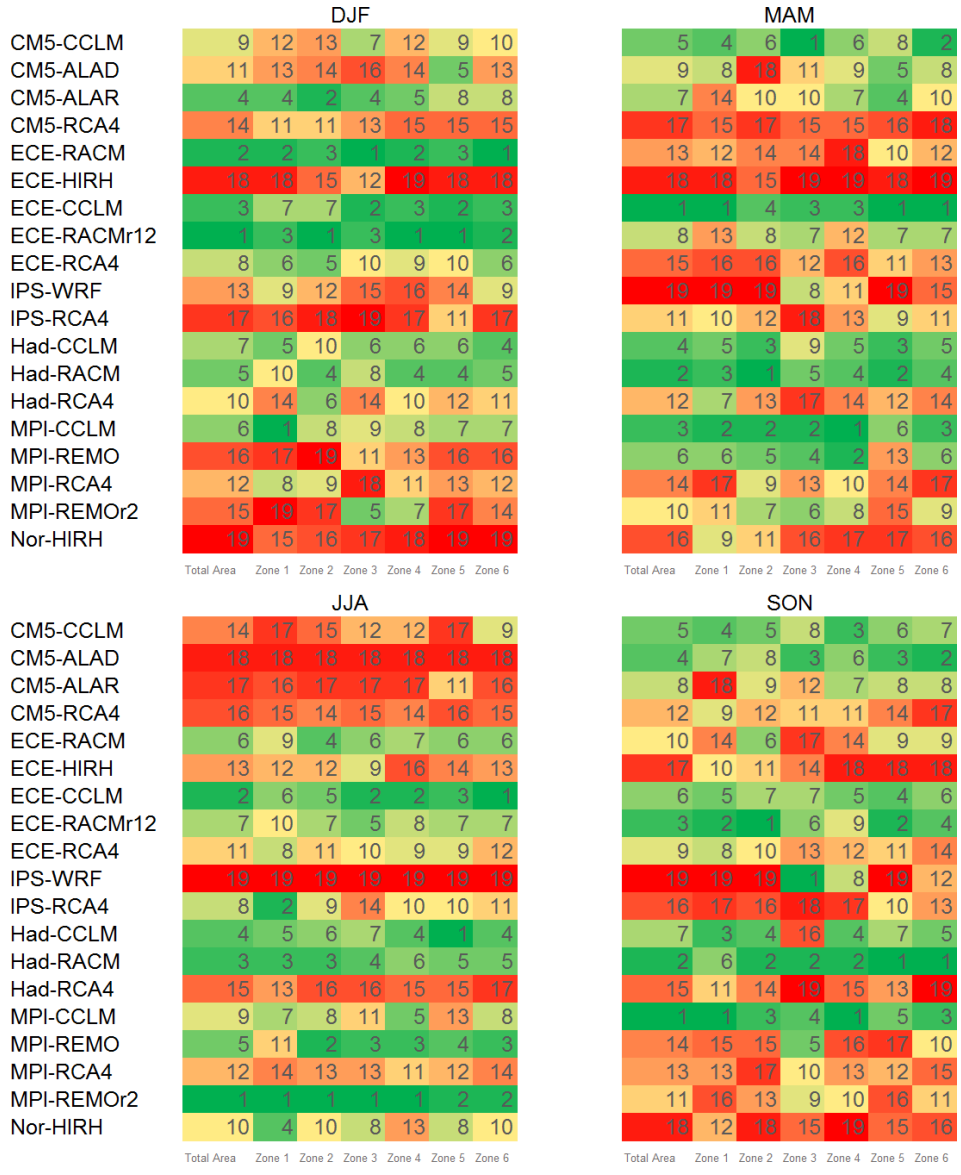

Figure 10. As Fig. 5 but for seasonal precipitation.

els looks rather similar, with limited errors until $L = 3$ years (± 0.5 years).

Finally, the models were also ranked according to their ability to reproduce both observed drought maximum intensities and return periods of drought events with duration $L = 3$ years (Fig. 14a). Drought intensity was selected as it merges drought accumulated deficit and duration of each drought event. Concerning the return period, it is worth pointing out that the choice of the considered drought duration only affects the magnitude of the errors, while the performance of each model with respect to the others does not change (see Fig. 12). As shown in Fig. 14a, the best models for the whole study area are confirmed to be ECE-CCLM, Had-RACM, ECE-RACM, and Had-CCLM. Interestingly, CM5-ALAR is the best model for Zone 3 but unsuitable for the remaining zones. The worst model for all the zones is CM5-RCA4, whereas poor performances are associated with ECE-RACMr12 for Zones 1 and 2, Had-RCA4 for Zone 3, MPI-REMOr2 for Zones 4 and 6, and IPS-WRF for Zone 5.

4.3.2 Seasonal scale

Figure 11d, e, and f represent the box plots of the errors related to maximum drought duration, accumulated deficit, and intensity identified on seasonal precipitation data.

Concerning drought duration (Fig. 11d), several models (9 out of 19) show a median error equal to 0, while the other models tend to underestimate, with the only exception being IPS-WRF. Overall, the errors span from -4 to $+3$ seasons.

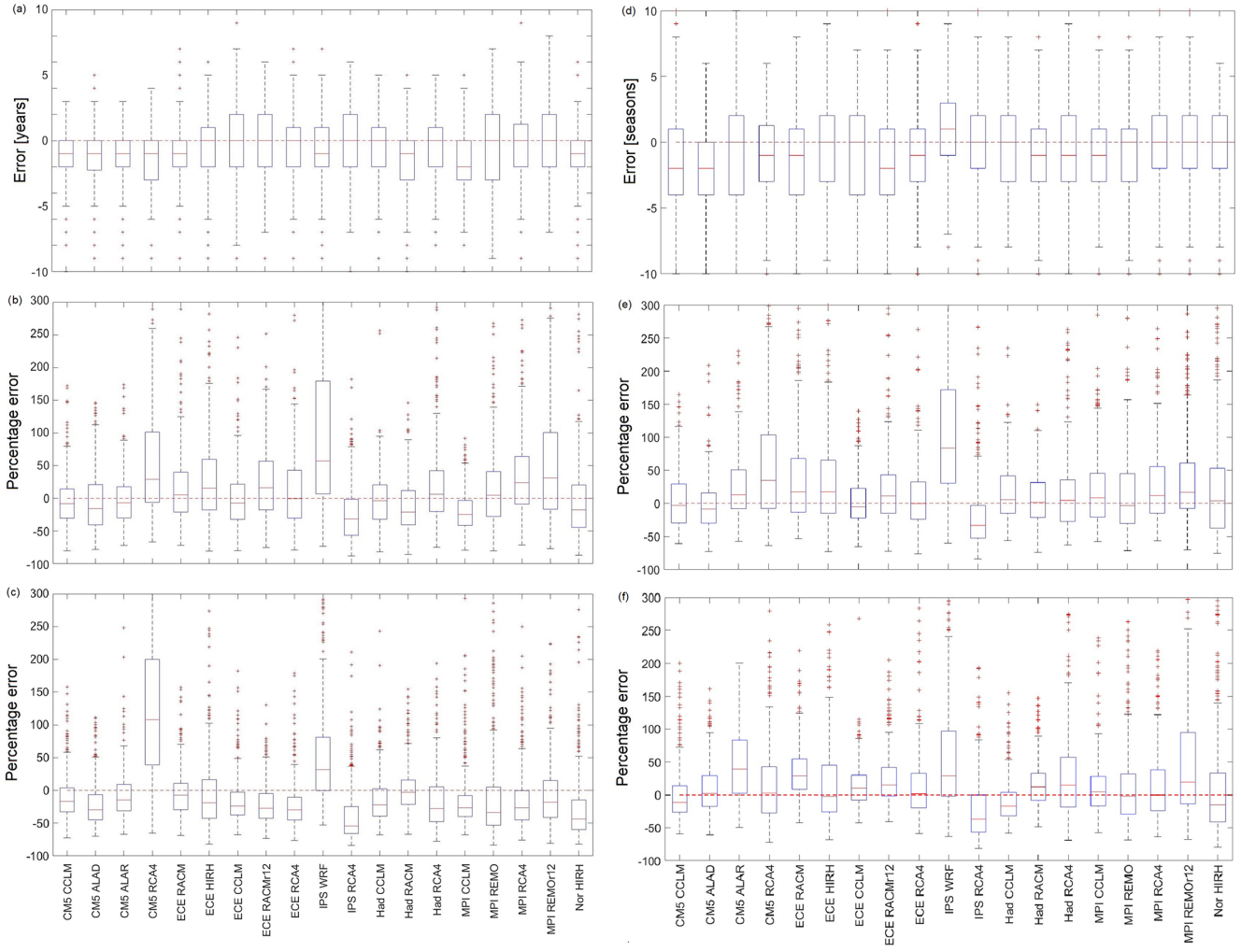

Figure 11. Box plots representing the frequency distribution of RCM percentage errors in **(a)** maximum drought duration (annual analysis), **(b)** maximum drought accumulated deficit (annual analysis), **(c)** maximum drought intensity (annual analysis), **(d)** maximum drought duration (seasonal analysis), **(e)** maximum drought accumulated deficit (seasonal analysis), and **(f)** maximum drought intensity (seasonal analysis).

The broadest IQR is associated with CMC5-ALAR and ECE-CCLM, while some models, such as IPS-RCA4, MPI-RCA4, MPI-REMOr2, and Nor-HIRH, seem equally reliable.

As for $D_{\max}$ (Fig. 11e), some similarities can be observed concerning the annual timescale (Fig. 11b) in terms of magnitude of percentage errors, although in the seasonal case most of the models tend to overestimate. The most reliable models are CM5-ALAD, ECE-CCLM, and Had-RACM. As for the annual scale, the least reliable is IPS-WRF, followed by CM5-RCA4 and Nor-HIRH.

Concerning $I_{\max}$, also in the seasonal case Had-RACM is confirmed as the best model, while MPI-REMOr2 and IPS-WRF are the worst (Fig. 11e). Once again, errors for this feature are less scattered than for accumulated deficit. Only four models underestimate $I_{\max}$, while most of the models are close to a zero median percentage error.

Figure 13 shows box plots of the errors in the return period of drought events of duration L equal to 2, 4, 6, and 8 seasons, respectively. In particular, the error was calculated as in Eq. (8) by replacing T_y with T_s, namely the return period of a drought event of fixed duration identified on seasonal data. As for the annual case, the performance of the models looks rather similar, with limited errors (± 5 seasons) until $L = 4$ seasons, with the exception of CM5-ALAD, CM5-ALAR, CM5-RCA4, and Had-RCA4.

Figure 14b illustrates the ranking of the models in reproducing the drought maximum intensities and return periods of drought events with duration $L = 4$ seasons. With respect to the annual scale, there is a certain agreement in identifying the best-performing models, which in this case are Had-RACM, Had-CCLM, and ECE-CCLM. In particular, Had-RACM performs well in every zone, while Had-CCLM is

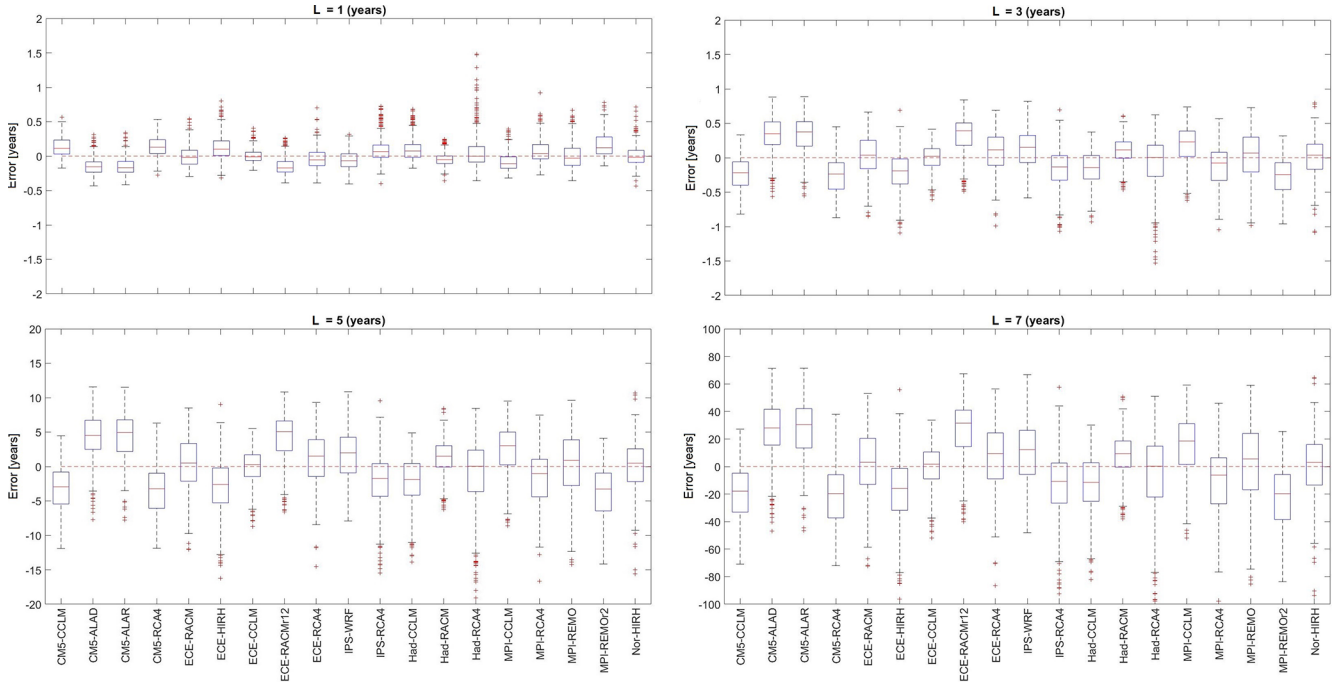

Figure 12. Box plots representing the frequency distribution of RCM errors in the return period of drought events of duration L equal to 1, 3, 5, and 7 years.

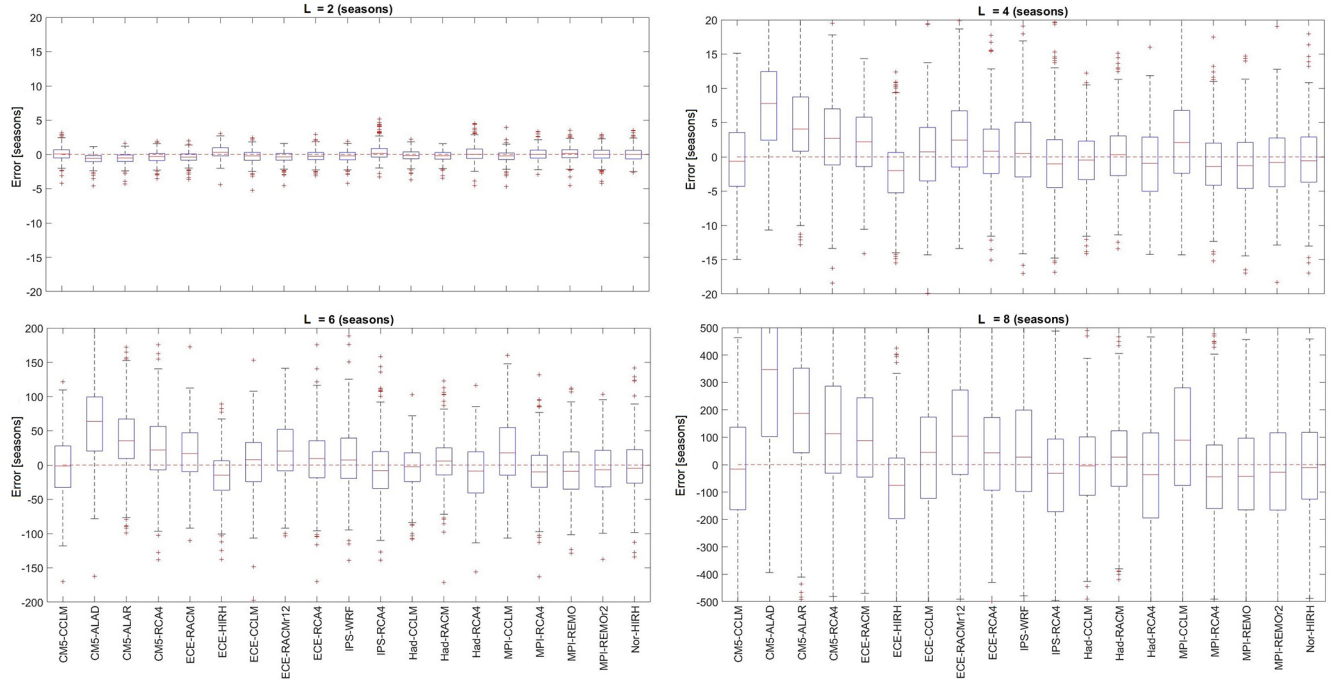

Figure 13. Box plots representing the frequency distribution of RCM percentage errors in the return period of drought events of duration L equal to 2, 4, 6, and 8 seasons.

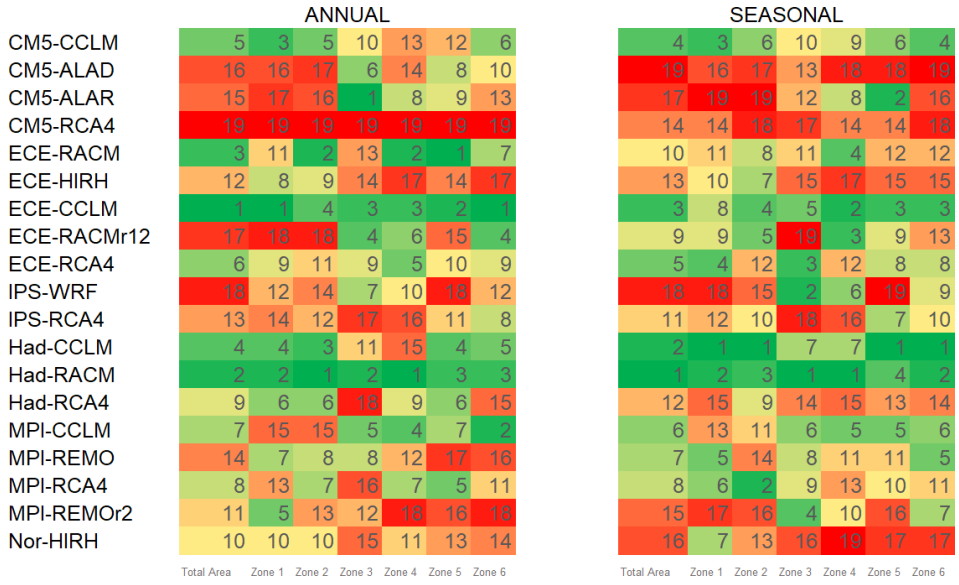

Figure 14. RCM ranking with respect to their ability to reproduce both observed drought maximum intensities and return periods of drought events with duration $L = 3$ years (left) and $L = 4$ seasons (right).

the best model for Zones 1, 2, 5, and 6. The worst-performing models are CM5-ALAD, CM5-ALAR (albeit it ranks second for Zone 5), CM5-RCA4, and Nor_HIRH.

5 Discussion

Table 6 illustrates the best-performing models according to the ranking approach for each of the considered variables over the whole area and the six homogeneous zones, respectively. In particular, the three best-performing models are reported for the mean temperature and precipitation inter-annual variability and drought intensity and return period of drought duration, while only the best CM for each season is indicated for seasonal variability.

It is worth underlining that the rankings are aimed at providing straightforward information about the relative accuracies of the models, e.g. for supporting the selection of a single or a few models in a specific area; therefore, for the sake of simplicity, they provide reduced information based on cardinal numbering. However, the actual performance of each CM compared to the others can be highlighted by looking closer at the ε_m values, which reflect and summarize the results provided by the box plots and the Taylor diagrams.

Two kinds of comparisons are carried out in this section: (1) on the same variable, across different timescales; (2) on the same timescale, across different variables. Further discussion is provided about relative impacts of different GCMs and RCMs, and, finally, an overall ranking is attempted aimed at providing a global evaluation of the CMs' performance.

5.1 Analyses across different timescales (inter-annual and seasonal)

Concerning temperature, the inter-comparison between the inter-annual and seasonal variability is rather straightforward. All the simulations are characterized by a more or less pronounced underestimation (Fig. 2a), together with a usually high correlation with observations (Figs. 2b and 4); i.e. both the observed inter-annual and seasonal variability are well reproduced. This is somehow confirmed by the rankings, where the relative differences among the models' performances are not very marked.

Conversely, in the case of precipitation, the performances of the models change significantly with the timescale. The most interesting case with this variable is CM5-ALAD, which, considering the total area, ranked 3rd for annual precipitation but provided low performances in most of the seasons (9th in MAM, 11th in DJF, and 18th in JJA). Though CM5-ALAD can reproduce relatively well the annual amount of rainfall, it is not as much able to simulate the seasonal variability; therefore the good performance at the annual timescale is due to the counterbalancing effects of the errors in different seasons. This feature of CM5-ALAD is amplified in several of the six zones, e.g. Zone 2 (where it is ranked 4th for the mean annual value but 14th in DJF and 18th in MAM and JJA) or Zone 6 (1st for the mean annual value but 13th in DJF and 18th in JJA). On the other hand, MPI-CCLM in the total area ranked eighth considering the annual precipitation but provided rather good results in single seasons (it is ranked third in MAM and first in SON).

However, considering the total area and the annual precipitation, the values of the error metric ε_m leading to the rank-

Table 6. Best-performing RCMs according to the ranking at the annual and seasonal scale.

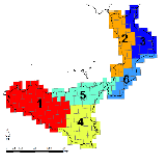

		Whole area	Zone 1	Zone 2	Zone 3	Zone 4	Zone 5	Zone 6
T interannual variability		MPI-REMO	MPI-REMO	MPI-CCLM	IPS-RCA4	MPI-CCLM	MPI-CCLM	IPS-RCA4
		MPI-CCLM	Had-CCLM	MPI-REMO	MPI-CCLM	MPI-REMO	MPI-REMO	MPI-REMO
		Had-CCLM	MPI-CCLM	Had-CCLM	Had-CCLM	Had-CCLM	Had-CCLM	MPI-CCLM
T seasonal variability	DJF	ECE-HIRH	CM5-CCLM	CM5-CCLM	ECE-HIRH	ECE-HIRH	MPI-CCLM	MPI-CCLM
	MAM	ECE-CCLM	ECE-CCLM	MPI-REMOr2	ECE-CCLM	MPI-REMOr2	ECE-CCLM	ECE-CCLM
	JJA	IPS-RCA4	IPS-RCA4	IPS-RAC4	Had-RCA4	IPS-RCA4	MPI-REMOr2	MPI-REMOr2
	SON	MPI-REMOr2	MPI-REMOr2	MPI-REMOr2	Had-CCLM	MPI-REMOr2	MPI-REMOr-12	MPI-CCLM
P interannual variability		Had-RACM	Had-RACM	ECE-RACM	ECE-CCLM	ECE-CCLM	ECE-CCLM	CM5-ALAD
		ECE-CCLM	CM5-CCLM	Had-RACM	Had-CCLM	Had-RACM	CM5-ALAD	Had-RACM
		CM5-ALAD	CM5-ALAD	CM5-ALAR	Had-RACM	Had-CCLM	Had-RACM	ECE-RACMr12
P seasonal variability	DJF	ECE-RACMr12	MPI-CCLM	ECE-RACMr12	ECE-RACM	ECE-RACMr12	ECE-RACMr12	ECE-RACM
	MAM	ECE-CCLM	ECE-CCLM	Had-RACM	CM5-CCLM	MPI-CCLM	ECE-CCLM	ECE-CCLM
	JJA	MPI-REMOr2	MPI-REMOr2	MPI-REMOr2	MPI-REMOr2	MPI-REMOr2	Had-CCLM	ECE-CCLM
	SON	MPI-CCLM	MPI-CCLM	ECE-RACMr12	IPS-WRF	MPI-CCLM	Had-RACM	Had-RACM
I + T_y(L=3 years) (annual scale)		ECE-CCLM	ECE-CCLM	Had-RACM	CM5-ALAR	Had-RACM	ECE-RACM	ECE-CCLM
		Had-RACM	Had-RACM	ECE-RACM	Had-RACM	ECE-RACM	ECE-CCLM	MPI-CCLM
		ECE-RACM	CM5-CCLM	Had-CCLM	ECE-CCLM	ECE-CCLM	Had-RACM	Had-RACM
I+T_s(L=4 seasons) (seasonal scale)		Had-RACM	Had-CCLM	Had-CCLM	Had-RACM	Had-RACM	Had-CCLM	Had-CCLM
		Had-CCLM	Had-RACM	MPI-RCA4	IPS-WRF	ECE-CCLM	CM5-ALAR	Had-RACM
		ECE-CCLM	CM5-CCLM	Had-RACM	ECE-RCA4	ECE-RACMr12	ECE-CCLM	ECE-CCLM

ings are not very different among the first nine models, the ε_m value of the model ranked ninth (i.e. CM5-ALAR) being only 37 % higher than the best. The difference with respect to the best ε_m value is lower than 50 % in DJF for the first seven models, in MAM for the first five models, in JJA for the first six models, and in SON for the first seven models. The models always providing (i.e. considering both the annual and the seasonal values) differences lower than 50 % with respect to the best ε_m value are Had-RACM, ECE-CCLM, and Had-CCLM.

Figure 15 shows a comparison between the ranking of inter-annual variability of annual precipitation and the average position in the ranking of seasonal precipitation. It highlights possible deviations of the performances of the models at different timescales (the higher the deviation, the higher the distance from the bisector). When considering the seasonal scale, the reduced performance of CM5-ALAD is evident, such as the better ranking of MPI-CCLM. In general, the best models, at both the inter-annual and the seasonal scale, are Had-RACM and ECE-CCLM, followed by the two versions of ECE-RACM and two other CCLM models (namely, MPI-CCLM and Had-CCLM, the latter being penalized by the relatively lower ranking in winter).

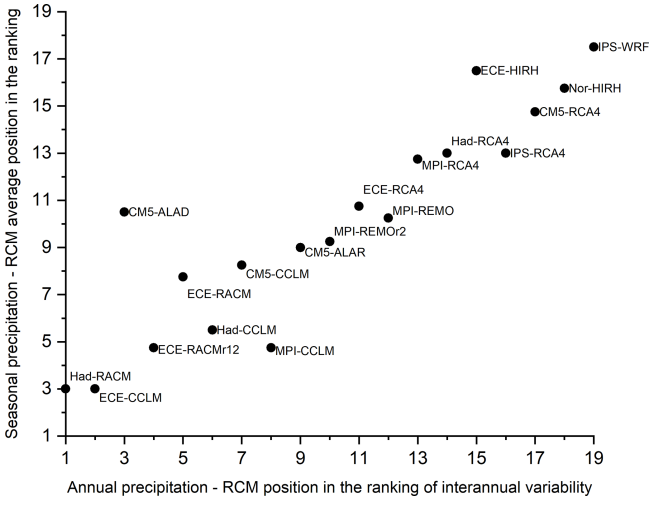

Figure 15. Comparison between the RCM position in the ranking of inter-annual variability of annual precipitation versus the average position in the ranking of seasonal variability of seasonal precipitation. Data concern the whole study area (Calabria and Sicily).

Focusing on drought analysis, box plots highlight a relevant variability in the frequency distribution of the error for all the considered drought characteristics. As for drought duration (Fig. 11a and d), the differences among the models appear more evident at the annual scale, while at the seasonal scale the models' behaviour looks rather similar. A general agreement can be observed between the box plots of drought accumulated deficit at the annual and the seasonal scale (Fig. 11b and e), where the IPS-WRF is confirmed as the worst model. Concerning drought intensity (Fig. 11c and f), CM5-RC4 provides a very poor performance at the annual scale, but a light improvement can be observed at the seasonal scale.

As for the return periods (Figs. 12 and 13), the seasonal scale emphasizes the poor quality of CM5-ALAD, which is also confirmed at the annual scale, together with CM5-ALAR, ECE-RACMr12, and MPI-CCLM.

Finally, the rankings combining the performance of the models to simulate maximum drought intensity and return period of drought events of fixed duration (Fig. 14a and b) agree in considering Had-RACM and ECE-CCLM as the best models at both the annual and seasonal scale.

5.2 Analyses across different variables

In terms of inter-annual variability, it is worth observing that, while MPI models appear the most suitable for mean temperature regardless of the area of investigation, especially regarding those in combination with REMO and CCLM RCMs, this is not the case for precipitation, although both the box plot and the Taylor diagram indicate some potential of the MPI-CCLM for precipitation (Fig. 6a and b). The box plots for both variables displayed a large spatial variability of the errors, suggesting the limited capacity of RCMs to properly capture spatial variations in both temperature and precipitation patterns. Regarding precipitation, a similar result was obtained by Mascaro et al. (2018) for the Sardinia region. To find a possible explanation, we decided to investigate possible relationships between the number of errors and the cells' mean altitude. In particular, correlation analyses between the elevation and the mean and the standard deviation of the mean annual air temperature and precipitation errors were carried out. Nonetheless, results, here not shown for the sake of brevity, did not provide significant correlations.

Turning to seasonal variability, some similarities between mean temperature and precipitation arise in spring, with the ECE-CCLM model looking valuable for both variables. ECE models also perform well in winter but in combination with different RCMs (i.e. HIRH for temperature and RACM for precipitation). In summer, the MPI-REMOr2 model is the best option for precipitation but works well also for mean temperature, mainly for Zones 5 and 6. In autumn, MPI-REMOr2 is once again the best-performing model but for mean temperature only. Alternatively, MPI-CCLM looks valuable for both mean temperature and precipitation during this season, as also confirmed by the Taylor diagrams (Figs. 4 and 9). Finally, the best models for drought intensity broadly recall those identified for annual precipitation, specifically for ECE-CCLM and Had-RACM.

The skills of CMs in reproducing drought characteristics and variability of precipitation are significantly linked. Drought characteristics, derived through the application of theory of runs, are functions of the departure from the thresholds rather than of the modelled precipitation itself. In other words, although a CM could significantly underestimate or overestimate annual and seasonal precipitation values (i.e. the data in the box plots in Figs. 6a and 8 may look loosely grouped and the medians very far from 0), it could still provide good performance in terms of drought characteristics simulation if it can reproduce time variability. It is interesting to observe that the distribution of the percentage error of drought intensity (Fig. 11c and f) is, in general, less scattered than that related to the accumulated deficit (Fig. 11b and e); therefore, one can conclude that a partial error compensation occurs when the modelled accumulated deficit is divided by the modelled duration. Despite the differences in the percentage errors, however, there is a general agreement in the identification of the best and, mainly, the worst models, also confirmed by the ranking of the models in reproducing drought intensity and return period of drought events with fixed duration (Fig. 14a and b) at both the annual and the seasonal timescale.

5.3 Impact of GCM and RCM choice and different realizations

Overall, no GCM prevails over the others because the RCMs deeply affect the final results. For example, concerning annual precipitation, the simulations relying on the Had GCM provide two high-ranked models (i.e. Had-CCLM and Had-RACM) and a low-ranked model (i.e. Had-RCA4). In the case of precipitation, only one among the GCMs used more than once coherently provides always bad results (IPS).

Concerning the most used RCMs, CCLM seems able to improve performances always with temperature (Fig. 3) and in most cases with precipitation (Fig. 7). Also, RACM usually provides high rankings with precipitation, while lower performances are found with temperature. The five occurrences of RCA4 very seldom provide high rankings with precipitation as well as the two occurrences of HIRH.

It is of some interest to analyse the behaviour of different realizations of the same CM, which provide insight into the effects of the variability of a multi-member GCM ensemble (von Trentini et al., 2019). In this study, two cases occur, i.e. ECE_RACM and MPI_REMO. Looking at all the box plots and Taylor diagrams, the two versions of the models behave rather coherently. Nevertheless, because of the variability of the overall model ensemble, they are usually not ranked in subsequent positions. For example, consider-

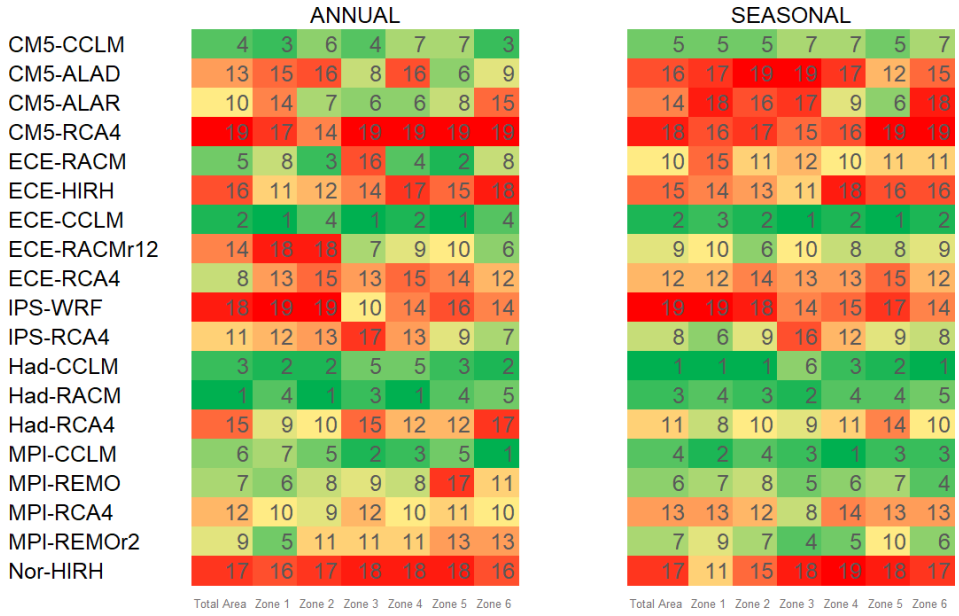

Figure 16. Overall ranking.

ing annual drought ranking and the total area, ECE-RACM is ranked 3rd and ECE-RACMr12 17th, while in the seasonal drought ranking MPI-REMO is ranked 7th and MPI-REMOr2 15th. This result highlights that, at least to a certain extent, the variability induced by different driving ensemble members is of the same order of the variability given by other GCM–RCM combinations. On the other hand, given the similar performances of the different realizations pointed out by the box plots and Taylor diagrams, it is confirmed that rather slight differences in models' performance can be found even for distances of four to five positions in the rankings.

5.4 Overall ranking and comparison with the literature

For a final evaluation of the models, an overall ranking criterion was applied. This ranking takes into consideration both the skills of the considered GCM–RCMs to replicate annual precipitation and temperature variability as well as drought characteristics. As shown in Fig. 16, the models with the best overall performances in both the whole case study area and in the six climatically homogeneous zones are those in combination with CCLM RCMs, with the significant exception of Had-RACM, which is ranked first considering the total area and Zones 2 and 4 for the annul timescale. Generally, the worst models at both the annual and the seasonal scale are Nor-HIRH, IPS-WRF, and CM5-RCA4, although at the seasonal scale also CM5-ALAD and CM5-ALAR have poor performances.

An attempt can be made to compare the results of our ranking exercise with similar studies. Such a comparison here is limited to the Euro-CORDEX climate models, for which, indeed, only a few studies exist. Perhaps the study from Kotlarski et al. (2014) allows the most interesting comparisons for our purposes, being focused on both precipitation and temperature at seasonal and yearly timescales and covering all areas of Europe, with specific results for the Mediterranean area. Models here denoted as CCLM (CLMCOM-11 in the mentioned study) perform well in reproducing annual temperature and precipitation in both studies. Differences arise for precipitation in the MAM season since CCLM models show poor performances according to Kotlarski et al. (2014), in contrast to our findings. Mascaro et al. (2018), whose study is focused on the Sardinia region (Italy), also found that the Had-RACM and ECE-CCLM models perform well in reproducing annual precipitation, while there is no agreement on the CM5-ALAD model. At the seasonal level, ECE-RACMr12, MPI-REMOr2, and MPI-CCLM perform well in both studies in the seasons DJF, JJA, and SON, respectively, while, in contrast to our results, in the MAM season the ECE-CCLM does not perform well. These differences in the ranking could be partially due to the different observational datasets used, which have been found to play a key role in climate model evaluations (Kotlarski et al., 2017).

6 Conclusions

In this study we compared the skill of 19 EURO-CORDEX RCMs at 0.11° ($\sim$ 12.5 km) grid spatial resolution in reproducing the annual and seasonal temperature and precipitation regime as well as several drought features observed in the period 1971–2000 in a dense network of rain gauges in Sicily and Calabria (southern Italy). From our investigation a few general and specific conclusions can be drawn.

From a general point of view, the model combinations are able to simulate temperature better than precipitation, even though important biases do exist in both variables. Models which are reliable in simulating precipitation may not be the same with respect to temperature. This is the case, for instance, with the ECE-RACM model, which is in the top ranks for precipitation while being in the lower ranks for temperature. Models that perform best for precipitation do almost the same for drought features. Differences between the rankings of annual with respect to seasonal characteristics do exist, but top-ranking models at the annual scale mostly perform well in a single season for both precipitation and temperature. Looking more specifically to the models, the Had-RACM, ECE-CCLM, Had-CCLM, and ECE-RACM are those that perform best for precipitation and drought, while the CM5-RCA4 and IPS-WRF are those that perform worst. For temperature, the models that perform best are MPI-CCLM, MPI-REMO, and Had-CCLM, while the worst are CM5-ALAD, ECE-RCA4, ECE-RACM, and CM5-RCA4. Had-CCLM performs well for both precipitation and temperature, while the CM5-RCA4 performs bad for both. Slight changes in models' performance occur when moving from the whole study area to the single zones, mainly at the seasonal scale. For instance, IPS-WRF is the best-performing model for Zone 3 (north-eastern Calabria) for seasonal precipitation in SON in contrast to what happens in the other zones. Differing behaviour of Zone 3 is also observed for drought investigations for CM5-ALAR and IPS-WRF models, respectively.

Results of this study reveal insight into RCM performances in small-scale regions, which are often targeted by impact studies and have so far received less attention, and provide some guidance to select the best models about the variable and the area under investigation. This is a key issue before addressing projection changes in the evolution of extreme hydro-meteorological events, such as drought characteristics (frequency, duration, and magnitude).

Data availability. Ground-based datasets are provided, upon request, by the "Centro Funzionale Multirischi – ARPACAL" (http://www.cfd.calabria.it/, Centro Funzionale Multirischi ARPACAL, 2020 – for Calabria) and the "Osservatorio delle Acque – Regione Sicilia" (http://www.acq.isprambiente.it/annalipdf/, ISPRA, 2020 – for Sicily). Climate data are freely available at the EURO-CORDEX website (https://www.euro-cordex.net/, EURO-CORDEX, 2020).

Supplement. The supplement related to this article is available online at: https://doi.org/10.5194/nhess-20-3057-2020-supplement.

Author contributions. AS, DJP, and BB designed the experiments. AS and BB contributed to sample preparation and preliminary data analysis. DJP and PN performed the main computations. AC and GM supervised the research. All authors discussed the results and contributed to the final paper.

Competing interests. The paper belongs to the special issue "Recent advances in drought and water scarcity monitoring, modelling and forecasting". Brunella Bonaccorso, co-author of the paper, is co-editor of the aforementioned special issue. Therefore, she did not assume the role of handling editor for this paper. The other authors declare that they have no conflict of interest.

Special issue statement. This article is part of the special issue "Recent advances in drought and water scarcity monitoring, modelling, and forecasting (EGU2019, session HS4.1.1/NH1.31)". It is a result of the European Geosciences Union General Assembly 2019, Vienna, Austria, 7–12 April 2019.

Acknowledgements. The authors thank the "Centro Funzionale Multirischi – ARPACAL" and the "Osservatorio delle Acque – Regione Sicilia" for providing the observed precipitation and temperature data. David J. Peres, Paola Nanni and Antonino Cancelliere acknowledge the EU LIFE 17 CCA/IT/000155 SimetoRES project (Urban adaptation and community learning for a resilient Simeto Valley).

Review statement. This paper was edited by Carmelo Cammalleri and reviewed by three anonymous referees.

References

Adeniyi, M. O. and Dilau, K. A.: Assessing the link between Atlantic Niño 1 and drought over West Africa using CORDEX regional climate models, Theor. Appl. Climatol., 131, 937–949, https://doi.org/10.1007/s00704-016-2018-0, 2018.

Arnell, N., Liu, C., Compagnucci, R., da Cunha, L., Hanaki, K., Howe, C., Mailu, G., Shiklomanov, I., Stakhiv, E., and Doll, P.: Hydrology and Water Resources, in: Climate Change2001: Impacts, Adaptation, and Vulnerability, edited by: McCarthy, J. J., Canziani, O. F., Leary, N. A., Dokken, D. J., and White, K. S., Cambridge University Press, Cambridge, UK, 192–234, 2001.

Baldauf, M., Seifert, A., Förstner, J., Majewski, D., Raschendorfer, M., Reinhardt, T., Baldauf, M., Seifert, A., Förstner, J., Majewski, D., Raschendorfer, M., and Reinhardt, T.: Operational Convective-Scale Numerical Weather Prediction with the COSMO Model: Description and Sensitivities, Mon. Weather Rev., 139, 3887–3905, https://doi.org/10.1175/MWR-D-10-05013.1, 2011.

Bentsen, M., Bethke, I., Debernard, J. B., Iversen, T., Kirkevåg, A., Seland, Ø., Drange, H., Roelandt, C., Seierstad, I. A., Hoose, C., and Kristjánsson, J. E.: The Norwegian Earth System Model, NorESM1-M – Part 1: Description and basic evaluation of the physical climate, Geosci. Model Dev., 6, 687–720, https://doi.org/10.5194/gmd-6-687-2013, 2013.

Bonaccorso, B., Cancelliere, A., and Rossi, G.: An analytical formulation of return period of drought severity, Stoch. Environ. Res. Risk Assess., 17, 157–174, https://doi.org/10.1007/s00477-003-0127-7, 2003.

Bonaccorso, B., Cancelliere, A., and Rossi, G.: Methods for Drought Analysis and Forecasting, in: Methods and Applications of Statistics in the Atmospheric and Earth Sciences, Hoboken, John Wiley and Sons, ISBN: 9780470503447, 150–184, 2012.

Bonaccorso, B., Peres, D. J., Cancelliere, A., and Rossi, G.: Large Scale Probabilistic Drought Characterization Over Europe, Water Resour. Manag., 27, 1675–1692, https://doi.org/10.1007/s11269-012-0177-z, 2013.

Bonaccorso, B., Peres, D. J., Castano, A., and Cancelliere, A.: SPI-Based Probabilistic Analysis of Drought Areal Extent in Sicily, Water Resour. Manag., 29, 459–470, https://doi.org/10.1007/s11269-014-0673-4, 2015a.

Bonaccorso, B., Cancelliere, A., and Rossi, G.: Probabilistic forecasting of drought class transitions in Sicily (Italy) using Standardized Precipitation Index and North Atlantic Oscillation Index, J. Hydrol., 526, 136–150, https://doi.org/10.1016/j.jhydrol.2015.01.070, 2015b.

Bordi, I. and Sutera, A.: An analysis of drought in Italy in the least fifty years, Nuovo Cimento C, 25, 185–206, 2002.

Cancelliere, A. and Salas, J.: Drought length properties for periodic stochastic hydrological data, Water Resour. Res., 10, 1–13, 2004.

Cancelliere, A. and Salas, J.: Drought probabilities and return period for annual streamflows series, J. Hydrol., 391, 77–89, 2010.

Centro Funzionale Multirischi ARPACAL: Dati Storici, available at: http://www.cfd.calabria.it/, last access: 6 November 2020.

Christensen, J. H., Kjellström, E. K., Giorgi, F., Lenderink, G., and Rummukainen, M.: Weight assignment in regional climate models, Clim. Res., 44, 179–194, 2010.

Christensen, O. B., Drews, M., Christensen, J. H., Dethloff, K., Ketelsen, K., Hebestadt, I., and Rinke, A.: The HIRHAM Regional Climate Model Version 5 (beta), Tech. Rep. 06-17, 5, 1–22, 2007.

Colin, J., Déqué, M., Radu, R., and Somot, S.: Sensitivity study of heavy precipitation in Limited Area Model climate simulations: influence of the size of the domain and the use of the spectral nudging technique, Tellus A, 62, 591–604, https://doi.org/10.1111/j.1600-0870.2010.00467.x, 2010.

Collins, W. J., Bellouin, N., Doutriaux-Boucher, M., Gedney, N., Halloran, P., Hinton, T., Hughes, J., Jones, C. D., Joshi, M., Liddicoat, S., Martin, G., O'Connor, F., Rae, J., Senior, C., Sitch, S., Totterdell, I., Wiltshire, A., and Woodward, S.: Development and evaluation of an Earth-System model – HadGEM2, Geosci. Model Dev., 4, 1051–1075, https://doi.org/10.5194/gmd-4-1051-2011, 2011.

Coordinated Downscaling Experiment – European Domain (EURO-CORDEX): EURO-CORDEX Data, available at: http://www.cfd.calabria.it/, last access: 6 November 2020.

Coppola, E., Giorgi, F., Rauscher, S. A., and Piani, C.: Model weighting based on mesoscale structures in precipitation and temperature in an ensemble of regional climate models, Clim. Res., 44, 121–134, 2010.

De Troch, R., Hamdi, R., Van de Vyver, H., Geleyn, J.-F., Termonia, P., Troch, R. De, Hamdi, R., Vyver, H. Van de, Geleyn, J.-F., and Termonia, P.: Multiscale Performance of the ALARO-0 Model for Simulating Extreme Summer Precipitation Climatology in Belgium, J. Climate, 26, 8895–8915, https://doi.org/10.1175/JCLI-D-12-00844.1, 2013.

Diasso, U. and Abiodun, B. J.: Drought modes in West Africa and how well CORDEX RCMs simulate them, Theor. Appl. Climatol., 128, 223–240, https://doi.org/10.1007/s00704-015-1705-6, 2017.

Di Virgilio, G., Evans, J. P., Di Luca, A., Olson, R., Argüeso, D., Kala, J., Andrys, J., Hoffmann, P., Katzfey, J. J., and Rockel, B.: Evaluating reanalysis-driven CORDEX regional climate models over Australia: model performance and errors, Clim. Dynam., 53, 2985–3005, https://doi.org/10.1007/s00382-019-04672-w, 2019.

Dufresne, J.-L., Foujols, M.-A., Denvil, S., Caubel, A., Marti, O., Aumont, O., Balkanski, Y., Bekki, S., Bellenger, H., Benshila, R., Bony, S., Bopp, L., Braconnot, P., Brockmann, P., Cadule, P., Cheruy, F., Codron, F., Cozic, A., Cugnet, D., de Noblet, N., Duvel, J.-P., Ethé, C., Fairhead, L., Fichefet, T., Flavoni, S., Friedlingstein, P., Grandpeix, J.-Y., Guez, L., Guilyardi, E., Hauglustaine, D., Hourdin, F., Idelkadi, A., Ghattas, J., Joussaume, S., Kageyama, M., Krinner, G., Labetoulle, S., Lahellec, A., Lefebvre, M.-P., Lefevre, F., Levy, C., Li, Z. X., Lloyd, J., Lott, F., Madec, G., Mancip, M., Marchand, M., Masson, S., Meurdesoif, Y., Mignot, J., Musat, I., Parouty, S., Polcher, J., Rio, C., Schulz, M., Swingedouw, D., Szopa, S., Talandier, C., Terray, P., Viovy, N., and Vuichard, N.: Climate change projections using the IPSL-CM5 Earth System Model: from CMIP3 to CMIP5, Clim. Dynam., 40, 2123–2165, https://doi.org/10.1007/s00382-012-1636-1, 2013.

Endris, H. S., Omondi, P., Jain, S., Lennard, C., Hewitson, B., Chang'a, L., Awange, J. L., Dosio, A., Ketiem, P., Nikulin, G., Panitz, H. J., Büchner, M., Stordal, F., and Tazalika, L.: Assessment of the performance of CORDEX regional climate models in simulating East African precipitation, J. Climate, 26, 8453–8475, https://doi.org/10.1175/JCLI-D-12-00708.1, 2013.

Foley, A. and Kelman, I.: EURO-CORDEX regional climate model simulation of precipitation on Scottish islands (1971–2000): model performance and implications for decision-making in topographically complex regions, Int. J. Climatol., 38, 1087–1095, https://doi.org/10.1002/joc.5210, 2018.

Gampe, D., Schmid, J., and Ludwig, R.: Impact of Reference Dataset Selection on RCM Evaluation, Bias Correction, and Resulting Climate Change Signals of Precipitation, J. Hydrometeorol., 20, 1813–1828, https://doi.org/10.1175/JHM-D-18-0108.1, 2019.

Giorgetta, M. A., Jungclaus, J., Reick, C. H., Legutke, S., Bader, J., Böttinger, M., Brovkin, V., Crueger, T., Esch, M., Fieg, K., Glushak, K., Gayler, V., Haak, H., Hollweg, H.-D., Ilyina, T., Kinne, S., Kornblueh, L., Matei, D., Mauritsen, T., Mikolajewicz, U., Mueller, W., Notz, D., Pithan, F., Raddatz, T., Rast, S., Redler, R., Roeckner, E., Schmidt, H., Schnur, R., Segschneider, J., Six, K. D., Stockhause, M., Timmreck, C., Wegner, J., Widmann, H., Wieners, K.-H., Claussen, M., Marotzke, J., and Stevens, B.: Climate and carbon cycle changes from 1850 to 2100 in MPI-ESM simulations for the Coupled Model Intercomparison Project phase 5, J. Adv. Model. Earth Sy., 5, 572–597, https://doi.org/10.1002/jame.20038, 2013.

Giorgi, F.: Climate change hot-spots, Geophys. Res. Lett., 33, 1–4, https://doi.org/10.1029/2006GL025734, 2006.

Giorgi, F. and Lionello, P.: Climate change projections for the Mediterranean region, Global Planet. Change, 63, 90–104, https://doi.org/10.1016/j.gloplacha.2007.09.005, 2008.

Gonzalez, J. and Valdes, J.: Bivariate drought recurrence analysis using tree ring reconstructions, J. Hydrol. Eng., 8, 247–258, 2003.

Harris, I., Jones, P. D., Osborn, T. J., and Lister, D. H.: Updated high-resolution grids of monthly climatic observations – the CRU TS3.10 Dataset, Int. J. Climatol., 34, 623–642, https://doi.org/10.1002/joc.3711, 2014.

Hart, O. E. and Halden, R. U.: On the need to integrate uncertainty into U.S. water resource planning, Sci. Total Environ., 691, 1262–1270, https://doi.org/10.1016/j.scitotenv.2019.07.164, 2019.

Haylock, M. R., Hofstra, N., Klein Tank, A. M. G., Klok, E. J., Jones, P. D., and New, M.: A European daily high-resolution gridded data set of surface temperature and precipitation for 1950–2006, J. Geophys. Res.-Atmos., 113, D20119, https://doi.org/10.1029/2008JD010201, 2008.

Hazeleger, W., Severijns, C., Semmler, T., Ştefănescu, S., Yang, S., Wang, X., Wyser, K., Dutra, E., Baldasano, J. M., Bintanja, R., Bougeault, P., Caballero, R., Ekman, A. M. L., Christensen, J. H., van den Hurk, B., Jimenez, P., Jones, C., Kållberg, P., Koenigk, T., McGrath, R., Miranda, P., van Noije, T., Palmer, T., Parodi, J. A., Schmith, T., Selten, F., Storelvmo, T., Sterl, A., Tapamo, H., Vancoppenolle, M., Viterbo, P., and Willén, U.: EC-Earth, B. Am. Meteorol. Soc., 91, 1357–1364, https://doi.org/10.1175/2010BAMS2877.1, 2010.

Huntington, T. G.: Evidence for intensification of the global water cycle: Review and synthesis, J. Hydrol., 319, 83–95, https://doi.org/10.1016/j.jhydrol.2005.07.003, 2006.

IPCC: Climate Change 2014: Synthesis Report. Contribution of Working Groups I, II and III to the Fifth Assessment Report of the Intergovernmental Panel on Climate Change, IPCC, Geneva, Switzerland, 151 pp., 2014.

IPCC: Global warming of 1.5°C. An IPCC Special Report on the impacts of global warming of 1.5°C above pre-industrial levels and related global greenhouse gas emission pathways, in the context of strengthening the global response to the threat of climate change, sustainable development, and efforts to eradicate poverty, edited by: Masson-Delmotte, V., Zhai, P., Pörtner, H. O., Roberts, D., Skea, J., Shukla, P. R., Pirani, A., Moufouma-Okia, W., Péan, C., Pidcock, R., Connors, S., Matthews, J. B. R., Chen, Y., Zhou, X., Gomis, M. I., Lonnoy, E., Maycock, T., Tignor, M., and Waterfield, T., Intergovernmental Panel on Climate Change, Geneva, Switzerland, 2018.

Istituto Superiore per la Protezione e la Ricerca Ambientale (ISPRA): Annali idrologici Storici, available at: http://www.acq.isprambiente.it/annalipdf/, last access: 6 November 2020.

Iversen, T., Bentsen, M., Bethke, I., Debernard, J. B., Kirkevåg, A., Seland, Ø., Drange, H., Kristjansson, J. E., Medhaug, I., Sand, M., and Seierstad, I. A.: The Norwegian Earth System Model, NorESM1-M – Part 2: Climate response and scenario projections, Geosci. Model Dev., 6, 389–415, https://doi.org/10.5194/gmd-6-389-2013, 2013.

Jacob, D., Petersen, J., Eggert, B., Alias, A., Christensen, O. B., Bouwer, L. M., Braun, A., Colette, A., Déqué, M., Georgievski, G., Georgopoulou, E., Gobiet, A., Menut, L., Nikulin, G., Haensler, A., Hempelmann, N., Jones, C., Keuler, K., Kovats, S., Kröner, N., Kotlarski, S., Kriegsmann, A., Martin, E., van Meijgaard, E., Moseley, C., Pfeifer, S., Preuschmann, S., Radermacher, C., Radtke, K., Rechid, D., Rounsevell, M., Samuelsson, P., Somot, S., Soussana, J.-F., Teichmann, C., Valentini, R., Vautard, R., Weber, B., and Yiou, P.: EURO-CORDEX: new high-resolution climate change projections for European impact research, Reg. Environ. Chang., 14, 563–578, https://doi.org/10.1007/s10113-013-0499-2, 2014.

Kjellström, E., Thejll, P., Rummukainen, M., Christensen, J. H., Boberg, F., Christensen, O. B., and Maule, C. F.: Emerging regional climate change signals for Europe under varying large-scale circulation conditions, Clim. Res., 56, 103–119, https://doi.org/10.3354/cr01146, 2013.

Kotlarski, S., Keuler, K., Christensen, O. B., Colette, A., Déqué, M., Gobiet, A., Goergen, K., Jacob, D., Lüthi, D., van Meijgaard, E., Nikulin, G., Schär, C., Teichmann, C., Vautard, R., Warrach-Sagi, K., and Wulfmeyer, V.: Regional climate modeling on European scales: a joint standard evaluation of the EURO-CORDEX RCM ensemble, Geosci. Model Dev., 7, 1297–1333, https://doi.org/10.5194/gmd-7-1297-2014, 2014.

Kotlarski, S., Szabó, P., Herrera, S., Räty, O., Keuler, K., Soares, P. M., Cardoso, R. M., Bosshard, T., Pagé, C., Boberg, F., Gutiérrez, J. M., Isotta, F. A., Jaczewski, A., Kreienkamp, F., Liniger, M. A., Lussana, C., and Pianko-Kluczyńska, K.: Observational uncertainty and regional climate model evaluation: A pan-European perspective, Int. J. Climatol., 39 3730–3749, 2017.

Llasat, M. C., Marcos, R., Turco, M., Gilabert, J., and Llasat-Botija, M.: Trends in flash flood events versus convective precipitation in the Mediterranean region: The case of Catalonia, J. Hydrol., 541, 24–37, 10.1016/j.jhydrol.2016.05.040, 2016.

Mascaro, G., White, D. D., Westerhoff, P., and Bliss, N.: Performance of the CORDEX-Africa regional climate simulations in representing the hydrological cycle of the Niger river basin, J. Geophys. Res., 120, 12425–12444, 2015.

Mascaro, G., Viola, F., and Deidda, R.: Evaluation of Precipitation From EURO-CORDEX Regional Climate Simulations in a Small-Scale Mediterranean Site, J. Geophys. Res.-Atmos., 123, 1604–1625, https://doi.org/10.1002/2017JD027463, 2018.

Mendicino, G. and Versace P.: Integrated Drought Watch System: A Case Study in Southern Italy, Water Resour. Manage., 21, 1409–1428, https://doi.org/10.1007/s11269-006-9091-6, 2007.

Meque, A. and Abiodun, B. J.: Simulating the link between ENSO and summer drought in Southern Africa using regional climate models, Clim. Dynam., 44, 1881–1900, https://doi.org/10.1007/s00382-014-2143-3, 2015.

Park, C., Min, S. K., Lee, D., Cha, D. H., Suh, M. S., Kang, H. S., Hong, S. Y., Lee, D. K., Baek, H. J., Boo, K. O., and Kwon, W. T.: Evaluation of multiple regional climate models for summer climate extremes over East Asia, Clim. Dynam., 46, 2469–2486, https://doi.org/10.1007/s00382-015-2713-z, 2016.

Peres, D. J., Caruso, M. F., and Cancelliere, A.: Assessment of climate-change impacts on precipitation based on selected RCM projections, European Water, E. W. Publications, 59, 9–15, 2017.

Peres, D. J., Modica, R., and Cancelliere, A.: Assessing Future Impacts of Climate Change on Water Supply System Performance: Application to the Pozzillo Reservoir in Sicily, Italy, Water, 11, 2531, https://doi.org/10.3390/w11122531, 2019.

Prein, A., Gobiet, A., Truhetz, H., Keuler, K., Goergen, K., Teichmann, C., and Nikulin, G.: Precipitation in the EURO-CORDEX

0.11° and 0.44° simulations: High resolution, high benefits?, Clim. Dynam., 46, 383–412, https://doi.org/10.1007/s00382-015-2589-y, 2016.

Rencher, A. C.: Multivariate Statistical Inference and Applications, John Wiley and Sons, INC., 559 pp., 1998.

Rockel, B., Will, A., and Hense, A.: The Regional Climate Model COSMO-CLM (CCLM), Meteorol. Z., 17, 347–348, https://doi.org/10.1127/0941-2948/2008/0309, 2008.

Rossi, G. and Benedini, M.: Water Resources of Italy. Protection, Use and Control; Springer International Publishing, 365 pp., 2020.

Schmidli, J., Goodess, C. M., Frei, C., Haylock, M. R., Hundecha, Y., Ribalaygua, J., and Schmith, T.: Statistical and dynamical downscaling of precipitation: An evaluation and comparison of scenarios for the European Alps, J. Geophys. Res.-Atmos., 112, D04105, https://doi.org/10.1029/2005JD007026m 2007.

Sen, Z.: Wet and dry periods of annual flow series, J. Hydraul. Div., 102, 1503–1514, 1976.

Senatore, A., Mendicino, G., Smiatek, G., and Kunstmann, H.: Regional climate change projections and hydrological impact analysis for a Mediterranean basin in southern Italy, J. Hydrol., 399, 70–92, 2011.

Senatore, A., Hejabi, S., Mendicino, G., Bazrafshan, J., and Irannejad, P.: Climate conditions and drought assessment with the Palmer Drought Severity Index in Iran: evaluation of CORDEX South Asia climate projections (2070–2099), Clim. Dynam., 52, 865–891, https://doi.org/10.1007/s00382-018-4171-x, 2019.

Senatore, A., Furnari, L., and Mendicino, G.: Impact of high-resolution sea surface temperature representation on the forecast of small Mediterranean catchments' hydrological responses to heavy precipitation, Hydrol. Earth Syst. Sci., 24, 269–291, https://doi.org/10.5194/hess-24-269-2020, 2020.

Smiatek, G. and Kunstmann, H.: Simulating Future Runoff in a Complex Terrain Alpine Catchment with EURO-CORDEX Data, J. Hydrometeorol., 20, 1925–1940, https://doi.org/10.1175/JHM-D-18-0214.1, 2019.

Smiatek, G., Kunstmann, H., and Senatore, A.: EURO-CORDEX regional climate model analysis for the Greater Alpine region: performance and expected future change, J. Geophys. Res.-Atmos., 121, 7710–7728, 2016.

Strandberg, G., Bärring, L., Hansson, U., Jansson, C., Jones, C., Kjellström, E., Kolax, M., Kupiainen, M., Nikulin, G., Samuelsson, P., Ullerstig, A., and Wang, S.: CORDEX scenarios for Europe from the Rossby Centre regional climate model RCA4, Report meteorology and climatology No. 116, Swedish Meteorological and Hydrological Institute (SMHI), ISSN: 0347-2116, 2014.

Taylor, K. E.: Summarizing multiple aspects of model performance in a single diagram, J. Geophys. Res.-Atmos., 106, 7183–7192, https://doi.org/10.1029/2000JD900719, 2001.

Taylor, K. E., Stouffer, R. J., and Meehl, G. A.: An overview of CMIP5 and the experiment design, B. Am. Meteorol. Soc., 93, 485–498, https://doi.org/10.1175/BAMS-D-11-00094.1, 2012.

Teichmann, C., Eggert, B., Elizalde, A., Haensler, A., Jacob, D., Kumar, P., Moseley, C., Pfeifer, S., Rechid, D., Remedio, A. R., Ries, H., Petersen, J., Preuschmann, S., Raub, T., Saeed, F., Sieck, K., and Weber, T.: How does a regional climate model modify the projected climate change signal of the driving GCM: A study over different CORDEX regions using REMO, Atmosphere, 4, 214–236, https://doi.org/10.3390/atmos4020214, 2013.

Torma, C., Giorgi, F., and Coppola, E.: Added value of regional climate modeling over areas characterized by complex terrain-Precipitation over the Alps, J. Geophys. Res.-Atmos., 120, 3957–3972, https://doi.org/10.1002/2014JD022781, 2015.

Um, M. J., Kim, Y., and Kim, J.: Evaluating historical drought characteristics simulated in CORDEX East Asia against observations, Int. J. Climatol., 37, 4643–4655, https://doi.org/10.1002/joc.5112, 2017.

Versace, P., Ferrari, E., Gabriele, S., and Rossi, F.: Valutazione delle piene in Calabria, Geodata, 30, 1989 (in Italian).

Voldoire, A., Sanchez-Gomez, E., Salas y Mélia, D., Decharme, B., Cassou, C., Sénési, S., Valcke, S., Beau, I., Alias, A., Chevallier, M., Déqué, M., Deshayes, J., Douville, H., Fernandez, E., Madec, G., Maisonnave, E., Moine, M.-P., Planton, S., Saint-Martin, D., Szopa, S., Tyteca, S., Alkama, R., Belamari, S., Braun, A., Coquart, L., and Chauvin, F.: The CNRM-CM5.1 global climate model: description and basic evaluation, Clim. Dynam., 40, 2091–2121, https://doi.org/10.1007/s00382-011-1259-y, 2013.

van Meijgaard, E., van Ulft, B., van de Berg, W. J., Bosveld, F. C., van den Hurk, B., Lenderink, G., and Siebesma, A. P.: The KNMI regional atmospheric climate model RACMO version 2.1 (KNMI TR-302), Tech. Rep., Technical Report TR-302, 2008.

van Vuuren, D. P., Edmonds, J., Kainuma, M., Riahi, K., Thomson, A., Hibbard, K., Hurtt, G. C., Kram, T., Krey, V., Lamarque, J. F., Masui, T., Meinshausen, M., Nakicenovic, N., Smith, S. J., and Rose, S. K.: The representative concentration pathways: An overview, Climatic Change, 109, 5–31, https://doi.org/10.1007/s10584-011-0148-z, 2011.

von Trentini, F., Leduc, M. and Ludwig, R. Assessing natural variability in RCM signals: comparison of a multi-model EURO-CORDEX ensemble with a 50-member single model large ensemble. Clim Dyn 53, 1963–1979, https://doi.org/10.1007/s00382-019-04755-8, 2019.

Wagner, S., Kunstmann, H., and Bardossy, A.: Uncertainties in water balance estimations due to scarce meteorological information: A case study for the White Volta catchment in West Africa, IAHS publication, 313, 86–97, 2007.

Wu, F. T., Wang, S. Y., Fu, C. B., Qian, Y., Gao, Y., Lee, D. K., Cha, D. H., Tang, J. P., and Hong, S. Y.: Evaluation and projection of summer extreme precipitation over east Asia in the regional model inter-comparison project, Clim. Res., 69, 45–58, 2016.

Yevjevich, V.: An objective approach to definitions and investigations of continental hydrologic droughtsm Hydrology paper 23, Colorado State University, Fort Collins, Colorado, 1967.